IOWA STATE UNIVERSITY
Digital Repository

Graduate Theses and Dissertations

Iowa State University Capstones, Theses and Dissertations

2016

Acceleration of percolation for cementitious sensors using conductive paint filler

Irvin Jude Joseph Pinto
Iowa State University

Follow this and additional works at: https://lib.dr.iastate.edu/etd

Part of the Civil Engineering Commons, Materials Science and Engineering Commons, and the Mechanics of Materials Commons

Recommended Citation
Pinto, Irvin Jude Joseph, "Acceleration of percolation for cementitious sensors using conductive paint filler" (2016). *Graduate Theses and Dissertations*. 15994.
https://lib.dr.iastate.edu/etd/15994

This Thesis is brought to you for free and open access by the Iowa State University Capstones, Theses and Dissertations at Iowa State University Digital Repository. It has been accepted for inclusion in Graduate Theses and Dissertations by an authorized administrator of Iowa State University Digital Repository. For more information, please contact digirep@iastate.edu.

Acceleration of percolation for cementitious sensors using conductive paint filler

by

Irvin Jude Joseph Pinto

A thesis submitted to the graduate faculty

in partial fulfillment of the requirements for the degree of

MASTER OF SCIENCE

Major: Civil Engineering (Civil Engineering Materials)

Program of Study Committee:

Simon Laflamme, Co-Major Professor
Kejin Wang, Co-Major Professor
Bora Cetin

Iowa State University

Ames, Iowa

2016

Copyright ©Irvin Jude Joseph Pinto, 2016. All rights reserved.

TABLE OF CONTENTS

LIST OF TABLES vi

NOMENCLATURE vii

ACKNOWLEDGMENTS viii

CHAPTER 1: INTRODUCTION AND BACKGROUND 1

1.1. Piezoelectric Composite Materials 1

1.2. Working Principle of Smart Materials 2

1.3. Percolation Thresholds in Composite Materials 4

1.4. Conductivity in Smart Materials 6

1.5. Smart Cementitious Materials 11

1.6. Accelerated Percolation in Conductive Polymer Composites 15

1.7. Contributions to Current Research 17

CHAPTER 2: REVIEW OF EXISTING LITERATURE 18

CHAPTER 3: MATERIALS AND FABRICAION OF SENSORS 27

3.1. Materials Used 27

3.1.1. Ball milling of carbon black 27

3.2. Fabrication of Sensors 29

3.2.1. Fabrication of sensors with carbon black only 29

3.2.2. Fabrication of sensors with carbon black and SEBS 30

3.3. Mix Proportions for CB and CB with SEBS Sensors....32

CHAPTER 4: TESTING AND EQUIPMENT....33

4.1. Impedance Measurements....33

4.1.1. Impedance v/s strain measurements....33

4.2. Measuring the quality of dispersion in the cementitious sensors....34

CHAPTER 5: RESULTS AND DISCUSSION....37

5.1. Percolation Plots....37

5.1.1. CB only sensors....37

5.1.2. CB with SEBS sensors....38

5.2. Effect of SEBS Loading on the Electrical Signal of Cementitious Sensors....39

5.3. Electrical Response to Applied Loading....41

5.3.1. Impedance v/s strain....41

5.4. Cyclic Loading with Constant Strain....45

5.5. Cyclic Loading with Varying Strains:....48

5.7. Compressive Strength....52

CHAPTER 6: CONCLUSIONS AND FUTURE SCOPE....59

REFERENCES....61

LIST OF FIGURES

Figure 1: Working principle of smart materials[3] 2
Figure 2: Resistive strain gauge working principle 2
Figure 3: Influence of nearby particles on the conductivity of the material [4] 5
Figure 4: A typical percolation threshold curve for Carbon fibers in cement [20] 7
Figure 5: An example of high structure carbon black with narrow enough distances for tunneling [4] 9
Figure 6: The equivalent circuit for two carbon black particles separated by a small gap [22] 10
Figure 7: Reinforcement mechanism of carbon nanotubes in hardened cement paste 12
Figure 8: Effects of carbon black on the compressive strength (a) and tensile strength (b) of cement paste composite [31] 13
Figure 9: Good and bad dispersion of carbon fibers [26] 13
Figure 10: Structure of SEBS 15
Figure 11: Selective localization of carbon black in polymer matrix [9] 16
Figure 12: Percolating networks of conductive filler in cement paste and (b) percolating networks of insulating aggregate in cement paste. [36] 17
Figure 13: Response of SWCNT films to static and dynamic loading [37] 18
Figure 14: Soft elastomeric capacitor with schematic [25] 19
Figure 15: Applied strain v/s measured stain for the SEC [25] 19
Figure 16: Test setup for strain reconstruction (left) and a schematic of the plate used (right) [23] 20
Figure 17: Percolation thresolds achieved with MWCNT's [2] 21
Figure 18: Change in resistivity for a static (a) and dynamic (b) case [47] 23
Figure 19: Compressive strength v/s CB loading in weight % [48] 24
Figure 20: Effect of carbon black on the compressive strength of PCC [50] 25
Figure 21: Selective localization of CB on PBD phase of an SBS copolymer [51] 26
Figure 22: Ball mill representation 27
Figure 23: Original CB 28
Figure 24: Ball milled CB after 15 hours with extremely fine particles 29
Figure 25: Representation of the fabrication procedure for CB only samples 30
Figure 26: Description of the SEBS Sensor fabrication process 31
Figure 27: Instron machine used to apply a strain controlled loading on the samples 33

Figure 28: Data acquisition system and laptop used to record the readings 34
Figure 29: 1.6% CB only before heating.....35
Figure 30: 1.6% CB only after 3 minutes of heating 35
Figure 31: 0.71% CB with SEBS before heating.....36
Figure 32: 0.71% CB with SEBS after 3 minutes of heating 36
Figure 33: CB only percolation 37
Figure 34: CB-SEBS percolation.....38
Figure 35: Combined percolation curves of CB only and CB with SEBS.....39
Figure 36: Resistivity v/s SEBS content for constant CB at 0.54% loading.....40
Figure 37: Percent change in Impedance v/s strain for 0.96% CB only samples 41
Figure 38: Percentage change in Impedance v/s strain for 0.54% CB with SEBS samples 42
Figure 39: Percentage change in strain for 0.71 42
Figure 40: Strain v/s Impedance for CB only samples before, within and after the percolation threshold 43
Figure 41: Strain v/s Impedance for CB with SEBS samples before, within and after the percolation threshold 44
Figure 42: Impedance v/s time for 0.54% CB with SEBS 46
Figure 43: Percent change in Impedance v/s time for 0.71% CB with SEBS.....46
Figure 44: Percent change in impedance v/s time for 0.96% CB only 47
Figure 45: Percent change in impedance v/s time for 1.6% CB only 47
Figure 46: Impedance v/s Time for 0.96% CB only sample 48
Figure 47: Change in impedance and strain v/s time for 0.54% CB with 9% SEBS.....49
Figure 48: Time v/s Impedance for 0.54% CB with SEBS sensors with 9%, 18% and 30% SEBS respectively. 50
Figure 49: Change in Impedance with time for varying temperature 51
Figure 50: Percent change in Impedance with time for varying temperature (Cement paste with SEBS) 52
Figure 51: Broken specimen of CB only showing all sides broken.....55
Figure 52: Broken specimens of CB with SEBS showing much less damage at failure 55
Figure 53: Strength v/s CB content for CB samples with SEBS 56
Figure 54: 28 days compressive strength 57
Figure 55: 7 days v/s 28 days compressive strength.....57

LIST OF TABLES

Table 1: CB only samples mix proportions 32
Table 2: CB with SEBS mix proportions 32
Table 3: Gauge factors of CB and CB with SEBS sensors 44
Table 4: Compressive strength of Samples with Cement only 53
Table 5: Compressive strength of Cement samples with SEBS 54

NOMENCLATURE

CB	Carbon Black
SEBS	Styrene-co-Ethylene-co-Butylene-co-Styrene
MWCNT	Multi Walled Carbon Nanotubes
CF	Carbon Fiber
PCC	Portland cement concrete
PP	Polypropylene
PS	Polystyrene
PBD	Polybutadiene
SEM	Scanning electron microscopy
SEC	Soft elastomeric capacitor

ACKNOWLEDGMENTS

I would like to thank my Co-Major Professors, Dr. Simon Laflamme and Dr. Kejin Wang, and committee member Dr. Bora Cetin, for their support and guidance throughout the project, and for keeping faith in me even when positive results were hard to come by. I am deeply grateful for their belief in me, which gave me tremendous motivation to complete my research, and I could not have asked for a better advisory committee.

Special thanks goes out to Dr. Joseph Schaefer at the Department of Aerospace Engineering for allowing me the use of the Instron machine to run compressive strain tests on our samples, and without which this research would be hard to complete in a timely manner. I would also like to thank Dr. Steve Holland at the Center for NonDestructive evaluation for his guidance and the use of the thermal camera from his research group, and Mr Robert Steffes for his guidance in using equipment in the Portland Cement Concrete research lab that helped me fabricate and test our cementitious sensors. A special mention goes out to my research group: Austin, Sijia, Liang, Liangyu, Sari, Hussam, Yuesheng, Laura and Alessandro for keeping me motivated and on track to complete and put together my research. Special thanks to Austin Downey and Hussam Saleem whose advice and tips helped solve quite a few obstacles in my research. I could not have done this without all of you.

Finally, I would like to thank my parents Eric and Joyce Pinto, and sister Gail, for the rock of support they have been for me for these two years of graduate study. To John and Diane Kubik, my parents away from home, for all your love, support and encouragement, and last but not least, Fleur Dias, for being that friend who never stopped telling me to believe in myself and who's pep talks kept me going when times were hard.

ABSTRACT

Structural health monitoring has emerged as an important branch of civil engineering in recent times, with the need to automatically monitor structural performance over time to ensure structural integrity. More recently, the advent of smart sensing materials has given this field a major boost. Research has shown that smart sensing materials fabricated with conductive filler at a concentration close to the percolation threshold results in high sensitivity to strain due to the piezoresistive effect. Of particular interest to this research are cementitious sensors fabricated using carbon black fillers. Carbon black is considered because of its widespread availability and low cost over other conductive fillers such as carbon nanotubes and carbon nanofibers. A challenge in the fabrication of these sensors is that cementitious materials require a significant amount of carbon black to percolate, resulting in a loss in mechanical properties. This research investigates a new method to accelerate percolation of the materials, enabling cementitious sensors with fewer carbon black particles. A carbon black-based conductive paint that allows earlier percolation by facilitating conducting networks in cementitious sensors is used. The conductive paint consists of a block copolymer, SEBS (styrene-co-ethylene-co-butylene-co-styrene), filled with carbon black particles. The percolation thresholds of sensors fabricated both with and without conductive paint are, as well as their strain sensing characteristics and compressive strength. The study found that SEBS could successfully reduce the percolation threshold by 42%, and that samples with SEBS showed better electrical responses in dynamic conditions. Despite showing lower compressive strength, cementitious sensors fabricated with this novel conductive paint show promise for real time health monitoring applications.

CHAPTER 1: INTRODUCTION AND BACKGROUND

1.1. Piezoelectric Composite Materials

Due to the growing need to continuously monitor the health of large-scale civil structures, there is a growing interest in the self-sensing potential of civil engineering materials. Of particular interest are the strain sensing characteristics of smart materials. Of particular interest are strain sensing capabilities of smart materials. These sensors are typically fabricated by adding conductive filler material into cementitious materials. Filler materials include carbon fibers, carbon nanotubes and carbon black. Piezoresistive cement based composites are considerably more robust when compared to many other composites and can easily be integrated with large structures. One major concern however, with such composites, is the addition of conducting filler considerably alters the physical properties of the material. In the case of cementitious materials, the addition of conductive filler materials like carbon black in large amounts have been known to make cement weaker [1]. While carbon nanotubes have been shown to actually increase the compressive and tensile strength of cement composites, their high costs, difficulty of dispersion in water and tendency to form agglomerates make them inconvenient to use [2]. Thus the challenging task for researchers is to find a filler material of low cost, which does not compromise the properties of the parent matrix.

1.2. Working Principle of Smart Materials

Smart mateials work on the principle that a change in dimensions due to applied strain results in a change in electrical properties for the material.

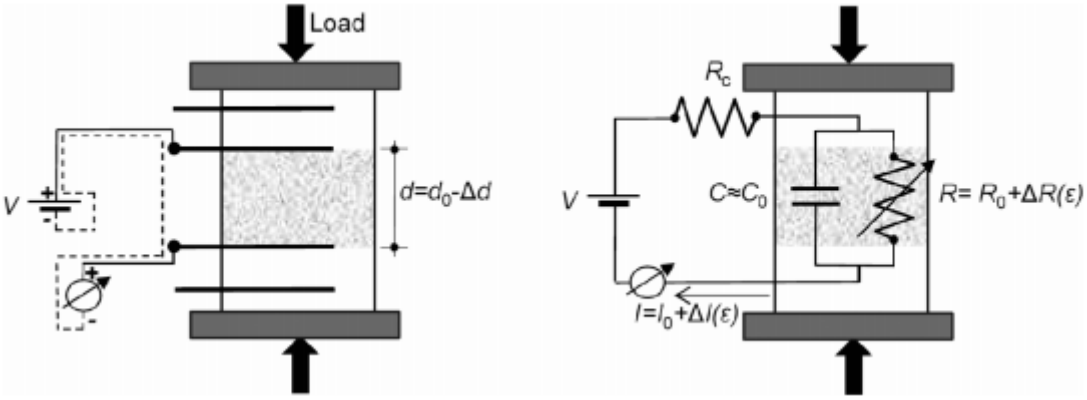

Figure 1: Working principle of smart materials[3]

The electromechanical model selected for the sensors is based off the working principle of RSG's (Resistive Strain Gauges). A resistive strain gauge can measure deformation based on a change in its length on the application of external strain.

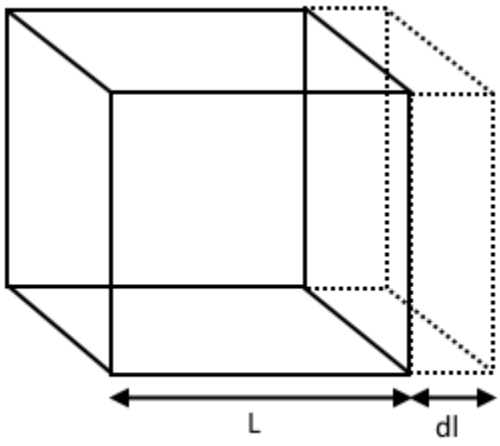

Figure 2: Resistive strain gauge working principle

Assume a square element of side L, with resistance R and area of cross section $A = l^2$

Its resistance, according to Ohm's law can be defined as $R = \rho\frac{L}{A}$ where ρ is the resistivity of the material.

Let the element be subjected to a small axial strain d σ. Taking the logarithm of the equation and assuming small changes in length, the derivative of this equation with respect to axial stress σ becomes

$$\frac{1}{R}\frac{dR}{d\sigma} = \frac{1}{\rho}\frac{d\rho}{d\sigma} + \frac{1}{l}\frac{dl}{d\sigma} - \frac{1}{A}\frac{dA}{d\sigma}$$

This can be re-written as

$$\frac{dR}{R} = \frac{d\rho}{\rho} + \frac{dl}{l} - 2\frac{dA}{A} \quad (1)$$

and the term $\frac{dL}{L}$ can be replaced as ϵ_l as the longitudinal strain

The axial stress also causes a change in cross section area, A. Taking the derivative of log of $A = l^2$ gives

$$\frac{dA}{A} = 2\frac{dl}{l}$$

$$\frac{dA}{A} = 2\epsilon_l$$

Where ϵ_t is the transverse strain on the element. This can be substituted in equation (1) as

which can be simplified to

$$\frac{dR}{R} = \frac{d\rho}{\rho} + \varepsilon_l - 2\epsilon_l$$

$$= \frac{d\rho}{\rho} + \varepsilon\mu$$

where $-\varepsilon_l$=μ

The sensitivity of various resistive elements differs based on material and electrical properties. This measure of sensitivity is known as the gauge factor of the resistive element defined as the change in resistance per unit applied strain or $\frac{dR/R}{\varepsilon}$. This is usually represented by λ.

$$\lambda = \frac{dR/R}{\varepsilon}$$

$$\lambda = \frac{\frac{d\rho}{\rho} + \varepsilon\mu}{\varepsilon}$$

and can be rewritten as

$$\lambda = \frac{\frac{d\rho}{\rho}}{\varepsilon} + \mu$$

$\frac{d\rho/\rho}{\varepsilon}$ is defined as the change in resistivity with strain or the piezoresistive component of the equation. This factor depends on the electrical properties of the material.

1.3. Percolation Thresholds in Composite Materials

Hardened cement paste without conducting materials is an insulator. The little conductivity seen is due to the conductivity of the cement matrix and the flow of free ions within the pore solution. Therefore, the resistivity of plain cement paste is high. On adding conductive filler material in low percentages and dispersing it well enough in the cement matrix, there is a very slight increase in the conductivity of the cement paste. However, this is not a substantial increase, since the isolated filler particles do not form chains or are not close enough to each other for charges to tunnel between neighboring conductive particles. However at a certain filler volume,

the conductive particles are now close enough to each other so that charges can jump or tunnel between adjacent neighbors [4]. This phenomenon is known as tunneling effect. Any slight increase in the percentage of filler material leads to a large increase in the conductivity as the conducting particles come closer together.

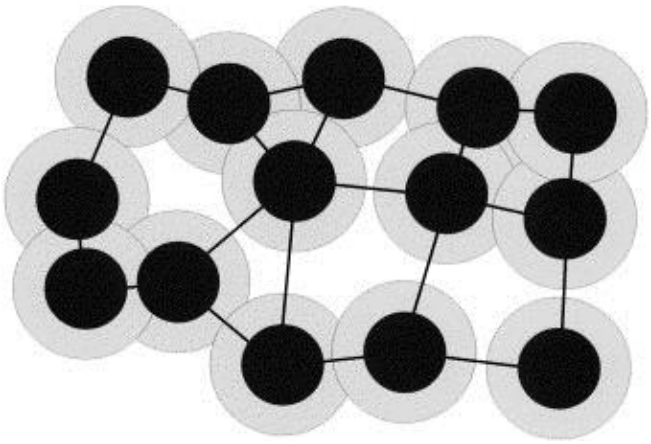

Figure 3: Influence of nearby particles on the conductivity of the material [4]

This volume fraction required to provoke a change in the materials phase from resistive to conductive yields the percolation threshold or region. At a certain volume fraction, conductive chains begin forming throughout the composite matrix and the composite makes a transition from an insulator to a conductor. Further addition of filler materials does not lead to large increases in the conductivity of the composite since conductive chains have already been formed. The percolation threshold for composite materials depends on many factors. This includes particle size [5][6], conductive filler type, mixing procedure speed [7] and dispersion states [8]–[10]. Particle size is important in determining the percolation characteristics of the composite. Research has shown that smaller particles lead to lowered percolation thresholds because of their ease of forming chains as the distance between particles is low when smaller particles are uniformly distributed in a composite matrix [5]. However, it is important that these particles form aggregates else there

could exist a scenario where small particles are dispersed evenly in a matrix and still not touch each other, and this is especially in the case of low structure spherical particles which can have percolation thresholds as high as 64% volume [4]. Thus particles that have a higher aspect ratio usually have lower percolation thresholds [11][2]. Rod shaped particles are more likely to touch each other and form conductive chains at lower volume fractions than spherical particles if they have the desired anisotropy in their dispersed state in the composite matrix. Polymer polarity was also shown to influence the percolation threshold where a more polar polymer reduces the percolation threshold [7], along with mixing times. A higher mixing time was shown to be detrimental to the filler-filler bonds in polymer matrixes despite leading to a better dispersion.

1.4. Conductivity in Smart Materials

The conductivity mechanisms proposed are mainly two theories, namely percolation theory and tunneling effect. Both these theories seek to explain the conduction mechanisms in composite smart materials. Percolation theory [12]–[15][16] can effectively explain conductivity mechanisms after percolation while tunneling effect theory [4], [15], [17]–[19] is used extensively to explain the electrical properties in the vicinity of the percolation threshold. Percolation theory states that at a certain volume fraction of filler materials, the formation of conducting chains occurs, and at this point, the composite makes a transition from an insulator to a conductor. A simple power law based on the statistical percolation equation has been formulated to explain this conductivity. The standard form of percolation theory is of the form

$$\sigma = \sigma_0 (\Phi - \Phi_C)^t$$

where Φ_C is the concentration of filler particles at percolation threshold, σ_0 is the conductivity of the filler material and t is the critical index of conductivity [13]. This equation is valid for

concentrations above the percolation threshold only, and is not used to explain conductivity before percolation is achieved.

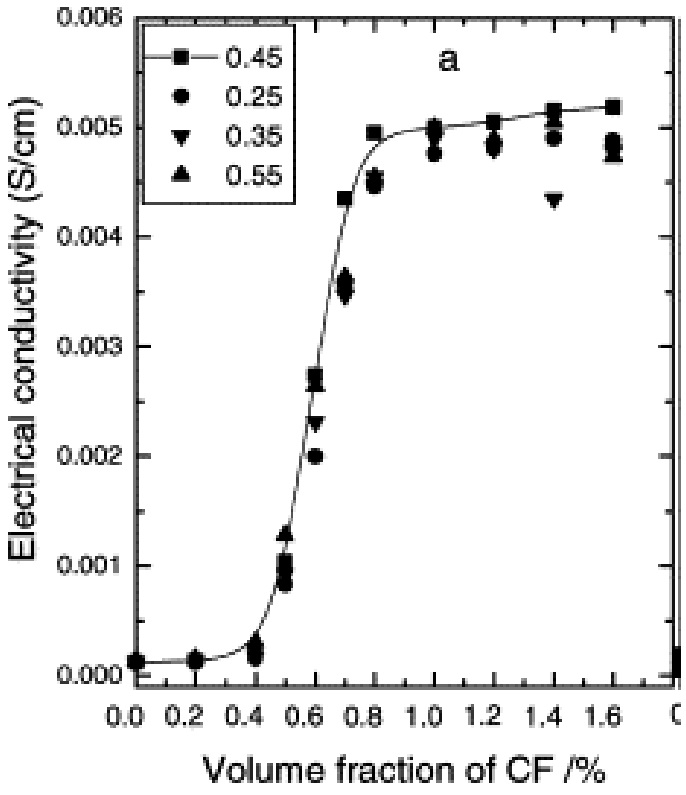

Figure 4: A typical percolation threshold curve for Carbon fibers in cement [20]

Tunnelling effect can be explained as followed. Initially, when the filler content is low, the conductivity seen is primarily due to that of the cement matrix. Since cement is more of an insulator, composite materials with low filler fractions show low conductivity. As filler material is added, the inter particle distances between filler particles decreases. At this particular point, electrons can jump or 'tunnel' through the narrow gap between two conductive filler particles. This phenomenon is known as tunnelling effect. Tunnelling effect needs two primary conditions to be satisfied. Firstly, the inter particle distances between two conductive particles should be small. Secondly, a high amount of energy needs to be transferred to the electrons so they can jump

or tunnel through the gap between conductive particles. A common equation that can be used to describe tunnelling is as follows:

$$j(\epsilon)=j_0 \exp[\frac{-\pi\chi w}{2}(\frac{\epsilon}{\epsilon_0}-1)^2] \quad (1)$$

where $j(\epsilon)$ is the tunnelling current across a gap with conductivity j_0 and with electric field ϵ. w is the gap width [4].

As the percentage of filler increases, conducting chains are formed. At a certain filler fraction, conductive chains are formed between the filler particles and the composite makes a transition from an insulator to a conductor. The filler volume that marks this transition is known as the percolation threshold for the material. The percolation equation is of the form $\sigma \propto (p-p_c)^t$ where p_c is the percentage of filler material that leads to percolation and t is a constant that determines the scaling behavior of the percolation curve in the region of p_c [21]. Studies have shown that the size and shape of the filler material plays an important role in the conductivity of the composite and will change the constants p_c and t. Clearly particles with an elongated and irregular shape will have lower pc values compared to more spherical particles, which would have higher values of pc and thus a higher percolation threshold. Filler materials with a low structure and which are more spherical in nature can essentially not touch each other even with high volume fractions of filler.

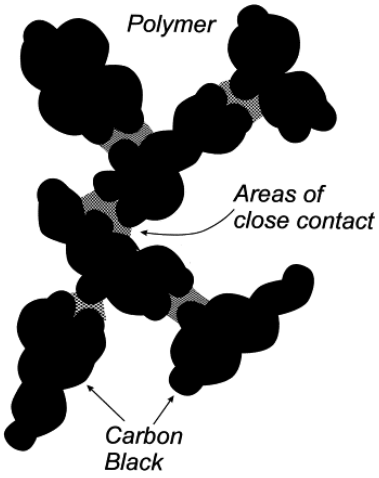

Figure 5: An example of high structure carbon black with narrow enough distances for tunneling [4]

Also the inter particle distance can remain significant for low structure filler materials. This can lead to a high value of t. However, high structure filler materials can considerably reduce inter particle distances and will hence have lower values of t. The value of t here is found to vary with the size of the conducting filler particles. Elongated particles tend to achieve better percolation thresholds as chances of contact between adjacent particles and formation of conductive networks are higher, however the particles need to have the required anisotropy in order to do so. Initial loading of filler materials does not lead to significant increase in conductivity, since there is an absence of continuous contact between filler materials at low concentration. However at higher concentrations, conductive chains are formed between conductive filler particles leading to a transition from an insulator to a conductor. The fraction of filler material required to cause this transition is known as the percolation threshold for the composite. At percolation, the flow of charge may either be through direct contact or due to tunneling effect. Studies on carbon black composites have shown the presence of tunneling effect between spheres of carbon black separated in a polymer or epoxy matrix. Since the carbon black particles do not come in contact with each

other, charge flow occurs due to the phenomenon of tunneling where electrons jump between the narrow insulating gaps between two adjacent spheres of carbon black.

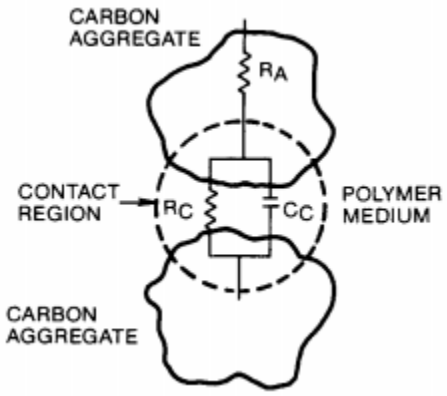

Figure 6: The equivalent circuit for two carbon black particles separated by a small gap [22]

If one were to try and model the above phenomenon when two carbon black particles are extremely close to each other, a possible model could be a resistor R_C and capacitor C_C in parallel, denoting the gap between the conductive particles, in series with R_A, the resistance of the conducting fibers [22]. At low AC frequencies, the value of impedance across this circuit will be relatively large, since the capacitive component blocks most of the current and the resistance comes from the large resistive component R_C. However at higher frequencies, the capacitor C_C acts almost like an open circuit, hence the current would bypass R_A and the corresponding impedance is much lesser than in the first case. As the loading of conductive particles is increased, R_C decreases and the net resistance R_A+R_C also decreases, thus increasing conductivity. Fabrication of sensors within the percolation threshold has been known to give a higher sensitivity to applied strain. [15] explained that within the percolation threshold, tunneling effect dominates the conduction mechanism of the composite materials and percolation theory governs the samples conductivity after percolation. Due to the nature of the tunneling equation, even a minor increase or decrease in the gap with

between conductive particles leads to a large change in conductivity in the composite. In the case of composites with conductive filler amounts in excess of the percolation threshold, tunneling no longer plays a significant effect and percolation theory dominates the conductivity mechanism, due to the formation of an infinite number of conducting networks. Thus, applying strain on samples with conductive particles well in excess of the percolation threshold will not cause a significant change in conductivity since netowrk formation is largely complete in these samples and there is very little tunneling taking place.

1.5. Smart Cementitious Materials

With the need to actively monitor the health of large-scale civil infrastructure, there is a need to better understand the self-sensing capabilities of civil engineering materials. Incorporation of conductive particles into cement and concrete can create a smart cementitious composite, with strain sensing capabilities. Some of the possible applications of these materials include weigh in motion sensors, strain gauges for bridge decks and slabs and weight sensors under roads for traffic light operations. Several research endeavors have been made in the field of smart materials in the field of structural health monitoring [3], [23]–[25].

The principles governing the conductivity of these composites are similar to what has been discussed above for polymer composites, however cementitious sensors bring upon the added complexity of dispersion, compatibility and the effect of microstructure development on the electrical and Piezoresistive properties of these composites. The conductive materials commonly used with Portland cement are carbon nanotubes [3], [26], [27], carbon fibers [27], [28] and carbon black [15], [18]. Also used are materials like Piezoresistive ceramics [29]. There are two advantages of adding carbon based conductive particles to cement paste. One of them is the increase in the toughness and fracture resistance of cement paste at low concentrations. Fibers

especially play an important role in controlling crack growth in cementitious materials. This phenomenon is not limited to carbon fibers alone but is also seen in glass fibers.

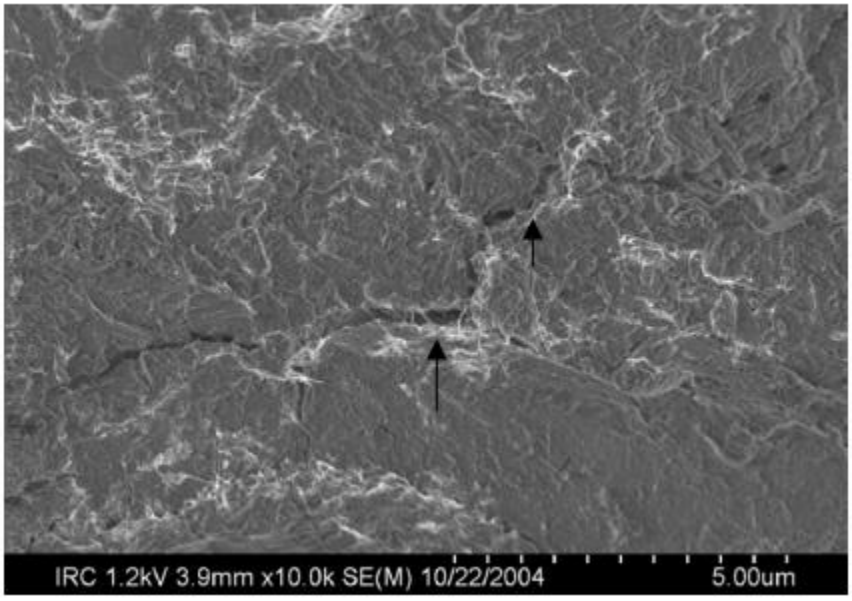

Figure 7: Reinforcement mechanism of carbon nanotubes in hardened cement paste

Fig 7 shows carbon nanotubes bridging cracks in cement paste. The carbon nanotubes are aligned approximately parallel to the cracks and appear to be controlling crack growth by provinding the tensile strength required to keep the crack under control. The above study also showed that carbon nanotubes increased the hardness of cement paste as compared to control samples [30]. Carbon black is also known to increase the compressive strength of cement pastes in low concentrations. This is because carbon black densifies the microstructure of cement and hence increases strength in low quantities . If the percentage of carbon black is increased too high, it can have the opposite effect on strength since it replaces cement by weight and hence reduces the amount of cementitious material in the mix. Research has shown that both the compressive as well as the tensile strength increases with moderate amounts of carbon black, but reduces with larger amounts of carbon black.

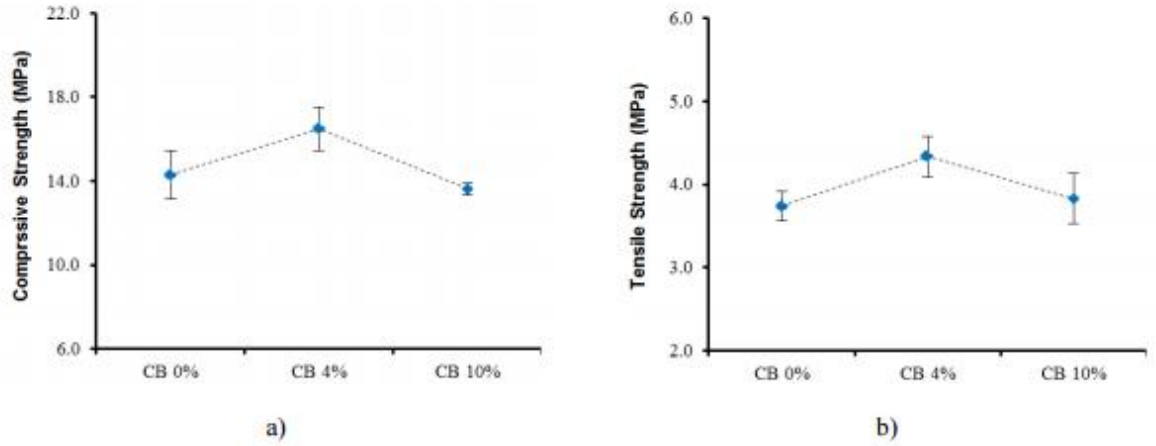

Figure 8: Effects of carbon black on the compressive strength (a) and tensile strength (b) of cement paste composite [31]

The dispersion of conductive fillers and fibers in cement matrix is important in achieving the right material and electrical properties. The electrical properties can be a good measure of the dispersion of conductive particles in the cement matrix. A good dispersion will lead to high conductivity while a poor dispersion leads to a poor conductivity due to the fact that the conductive particles, especially fibers, tend to form agglomerates together in bunches instead of forming continuous chains [32]. An illustration of this is shown in Fig 9.

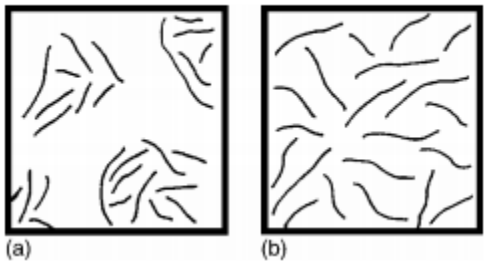

Figure 9: Good and bad dispersion of carbon fibers [26]

The idea of dispersion of fibers in cement should be to create continuous chain of fibers to allow for conductivity while at the same time allowing the fibers to be uniformly dispersed in the cement matrix. Agglomeration of fibers to a certain extent is desirable to ensure faster electrical percolation. There are several additives that can increase the degree of dispersion of conductive particles in a cement matrix. Silica fume, acrylic dispersions and methylcellulose have long been known to increase the dispersion of fibers in cement [33]. The improvement in the dispersion comes from the improvement of the interface between the conductive particles and cement.

Cementitious composites differ significantly from polymer composites due to the complex structure of hardened cement paste. The microstructure and pore fluid also play an important role in the conductivity of the cementitious composite. As the microstructure of cement develops, the pore fluid ionic concentration significantly changes, and the tortuosity of the pores increases as well. Therefore the microstructure development has a significant effect on the final electrical properties of cement. A polymer can also significantly alter the microstructure of cement.

Temperature has also been known to play a significant effect on the electrical properties of cement pastes. Increasing temperatures have shown to decrease the activation energy needed for the conduction process through cement pastes. Also affected is the pore water ionic concentration at increased temperatures which can lead to variations in conductivity [34].

1.6. Accelerated Percolation in Conductive Polymer Composites

The main motive behind this study was to accelerate percolation in cementitious sensors with the help of a block co-polymer. The copolymer used in the case of this study was SEBS (Styrene-co-Ethylene-co-Butylene-co-Styrene). SEBS has chains of styrene, ethylene and butylene, which are all immiscible. The aim was to get carbon black particles to agglomerate at the interface of these immiscible phases of SEBS, and hence form chains at a lower percentage than traditional CB cementitious sensors without the added polymer. The aim was to use as little SEBS as possible, as its purpose was solely to carry the CB through the cement matrix. Studies have shown success with this method of accelerated percolation.

Structure of Triblock Polymer (SEBS)

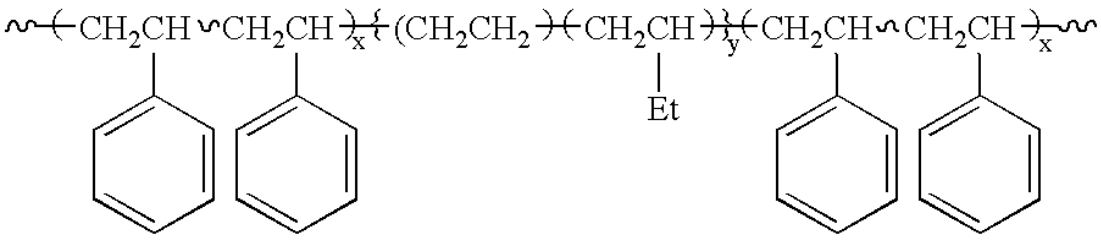

Figure 10: Structure of SEBS

In order to achieve earlier percolation, the carbon black is first dispersed in SEBS. Since SEBS is a copolymer with immiscible phases of Styrene, Ethylene and Butylene, the carbon black localizes at the boundaries of the two immiscible phases of polymer and hence can form chains faster due to selective localization [9][10][35]. It is this reason that SEBS and other block polymers are useful in reducing percolation thresholds.

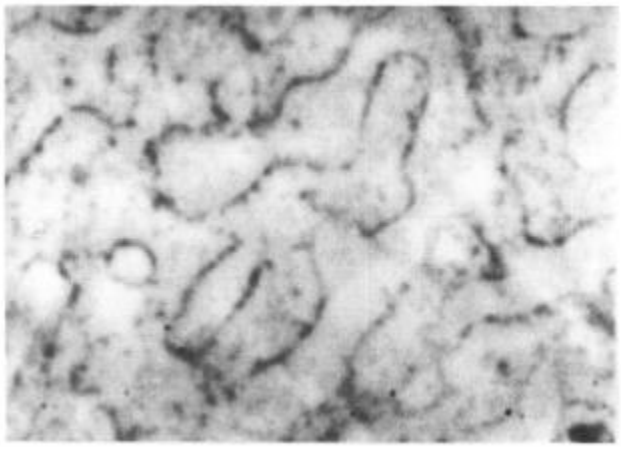

Figure 11: Selective localization of carbon black in polymer matrix [9]

Fig 11 shows carbon black localizing on the polypropylene phase of a Polypropylene-Polystyrene polymer blend. This preferential location of carbon black on the interface of two immiscible polymer blends occurs because of the surface tension between the two polymers and carbon black. CB particles prefer to be at the interface of the polymers which it has the lowest amount of surface tension with. The presence of SEBS also leads to another phenomenon called double percolation. Normally, in a composite containing just cement paste and conductive particles, the conductive particles will percolate at the concentration where enough conducting networks are formed through the cement paste matrix. Due to the presence of an insulator, SEBS, the percolation threshold is not only dependent on the amount of conductive particles added to the matrix but also the amount of insulating polymer added. SEBS being an insulator will block the flow of charges through the cement paste if present in large quantities. Thus, there exists an optimal amount of SEBS above which the sample will have a high value of electrical resistance. This can be illustrated by assuming a matrix of cement and aggregate. As the amount of aggregate (an insulator) increases, it would decrease

the conductivity of the cement paste, having exactly the opposite effect of a conductive filler.[36]

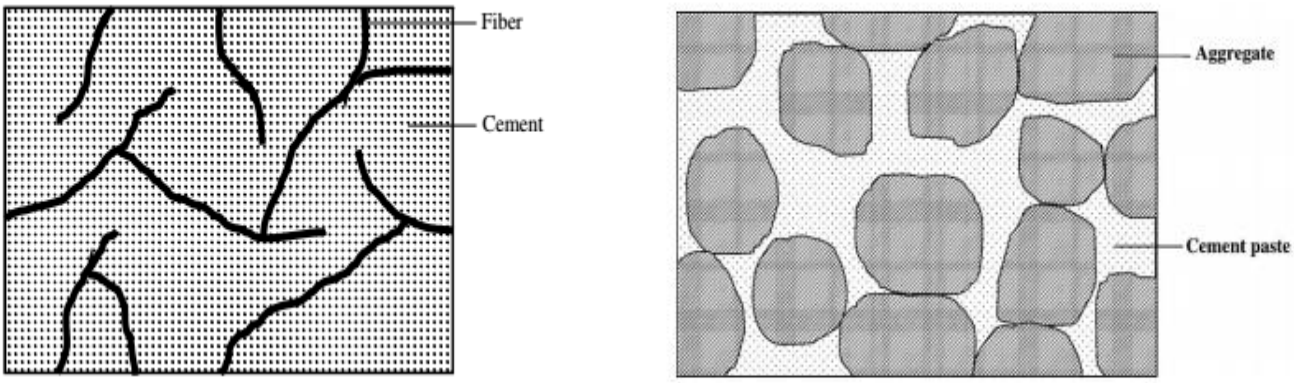

(a) (b)

Figure 12: Percolating networks of conductive filler in cement paste and (b) percolating networks of insulating aggregate in cement paste. [36]

1.7. Contributions to Current Research

Cementitious sensors with carbon black are a much cheaper alternative to using fillers like carbon nanotubes, despite having lower conductivity and lower structure. A simple solution to the above problem would be to accelerate percolation of carbon black in hardened cement paste. Using SEBS as a polymer to selectively localize CB is an efficient method of achieving the above objective. Introducing SEBS into cement paste would bring in challenges in dispersion of conductive paint and hydration of cement paste, which have been investigated in this study. A novel method of gauging dispersion of conductive filler in cementitious sensors using a current source to heat up the sample and a thermal camera to capture the heating pattern was also investigated, and was found to be an efficient alternative to SEM(Scanning electron microscopy).

CHAPTER 2: REVIEW OF EXISTING LITERATURE

Much of the existing literature on conductive composites as piezoresistive materials focuses on polymer composites. These studies include the electrical properties, studies on the percolation thresholds of polymer composites and their strain sensing properties. One interesting study focused on a stretchable carbon nanotube skin for human motion detection [37]. The authors employed thin SWCNT films cast on thin substrates which could be attached on clothing. The films of SWCNT were subjected to single and repeated loading and their response to strain was recorded. The authors reported that strain up to 280% could be measured using these thin films which was more than a conventional strain gauge could measure.

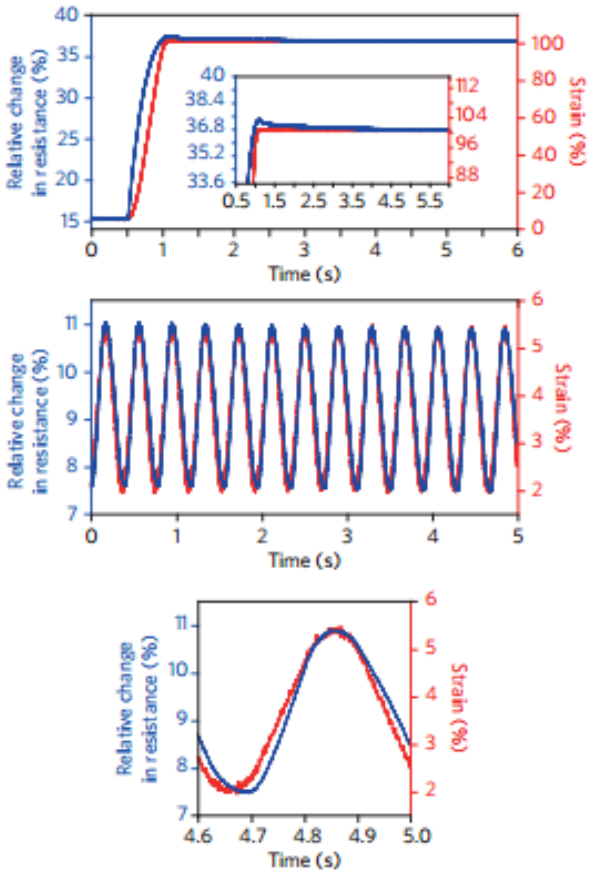

Figure 13: Response of SWCNT films to static and dynamic loading [37]

In the civil engineering domain, research on conductive polymer composites was done by Laflamme et al. [25] who developed a soft elastomeric capacitor capable of detecting and localizing damage on surfaces. This sensor was tested on a wind turbine blade and data suggested that the soft elastomeric capacitor had the potential to outperform traditional strain gauges as it provided additive strain measurements without any directional inputs.

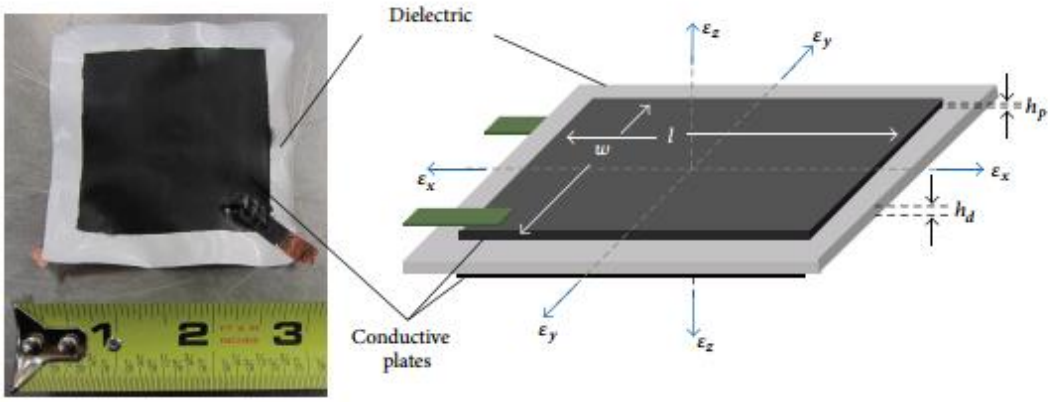

Figure 14: Soft elastomeric capacitor with schematic [25]

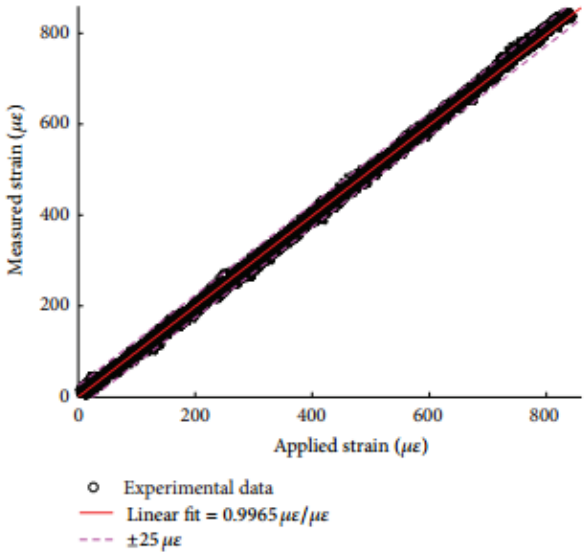

Figure 15: Applied strain v/s measured stain for the SEC [25]

As seen from Fig 15, the fit from these sensors was linear and matched the applied strain. Wu et al. [23] attempted to reconstruct surface strain using SEC's. An algorithm was used to decompose the additive in plane strain measurements from the SEC's into their principle components and a LSE(least square estimator) reduces the error between the assumed model and the SEC signals.

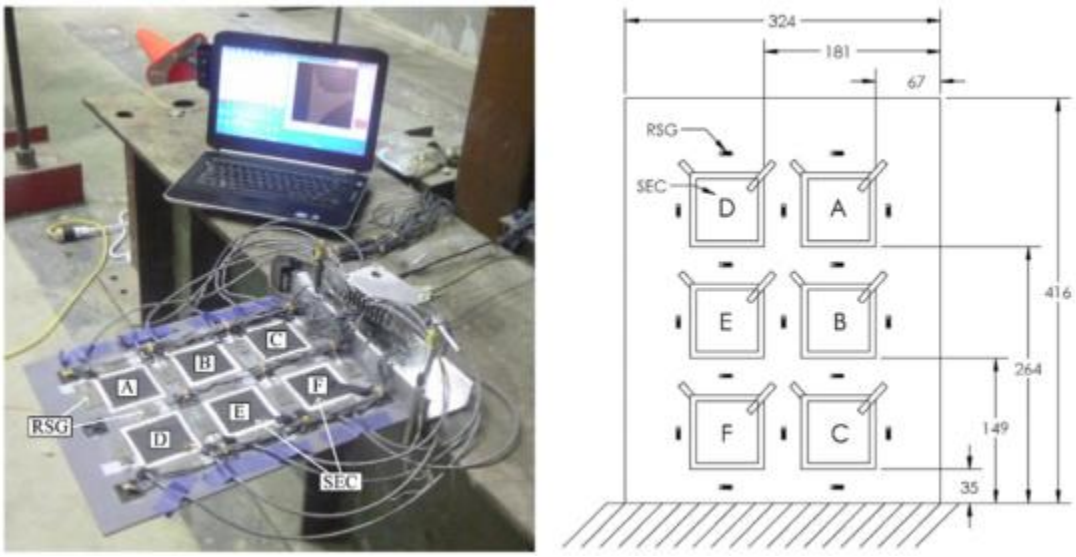

Figure 16: Test setup for strain reconstruction (left) and a schematic of the plate used (right) [23]

The electrical properties of carbon black-polymer composites were studied in depth by [4] who developed a model to determine the electrical properties of polymer composites with carbon black. It was discovered that when particles are within a close enough proximity, charges could tunnel through the gaps between conductive particles. Also discussed was the effect of the shape of the particles on the percolation threshold, another factor that is increasingly studied for the understanding of the conductive mechanisms in composites. A study by [5] found that smaller particles should lead to lowered percolation thresholds due to the fact that smaller particles can come into contact and form aggregates of chains more readily than larger particles. The authors

used a simple cubic lattice arrangement to show that the inter-particle distance was directly proportional to the particle size given below:

$$\delta = D\left[\left(\frac{\pi}{6\varphi}\right)^{1/3} - 1\right]$$

Where D is the diameter of the particles and δ is the interparticle gap.

A lot of research has been done with composites containing carbon nanotubes, due to their high aspect ratio and ability to form agglomerates and chains. Carbon nanotubes have been shown to achieve low percolation thresholds with epoxy [2]. The agglomeration of carbon nanotubes during the fabrication process was discussed, along with thermal effects on the arrangement of fibers.

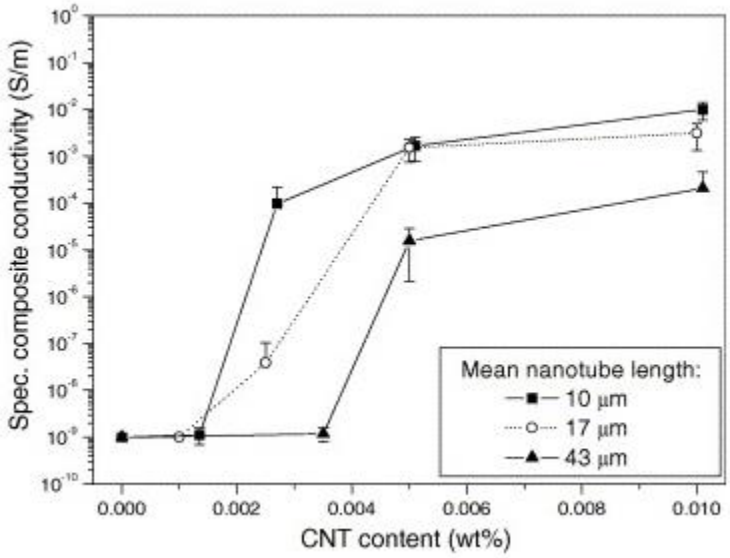

Figure 17: Percolation thresolds achieved with MWCNT's [2]

Low percolation thresholds of 0.005% were achieved using this method as seen from Fig 17. Carbon nanotubes were compared to carbon black [38] for their rheological and electrical properties, and it was shown that carbon nanotubes did lead to lowered percolation thresholds

when compared to carbon black. This could possibly be because of the shape and aspect ratio of carbon nanotubes as compared to carbon black.

The study of the self-sensing capabilities of civil engineering materials is a relatively unexplored field, but has seen recent growing interest. Most of the literature deals with conductive fibers and fillers incorporated into cement concrete [18], [27], [39]–[41], while there is also studies focused on the self-sensing characteristics of asphalt composites [42]–[46].

D'Alessandro et al. [3] modelled a cementitious sensor fabricated with MWCNT's and observed its response to dynamic loading. The cementitious sensors were mounted on a large beam and a dynamic load was applied. The strain sensing characteristics of the sensors were studied and it was found that the sensors had static and dynamic strain sensing capabilities, as well as being able to capture vibration signatures, thus proving to be useful for a number of civil engineering applications. Azhari et al. [27] investigated the strain sensing ability of carbon fibers and carbon nanotubes when incorporated into cement. Experiments over cyclic loading indicated that the changes in resistivity mimic both the loading and applied strain. Other studies showed that carbon fibers are more effective at sensing strain than steel fibers which were smaller in diameter (15μm v/s 8μm) and that smaller fibers were almost ineffective in creating piezoresistive cementitious composites [41]. Han et al. [47] studied the repeatibility of CB and CF based cementitious sensors and found the results to be repeatable and linearly variable with applied strain. Both static and cyclic loading cases were studied and the authors concluded that the sensors were effective in detecting strain upto 476 με and loadings up to 8MPa.

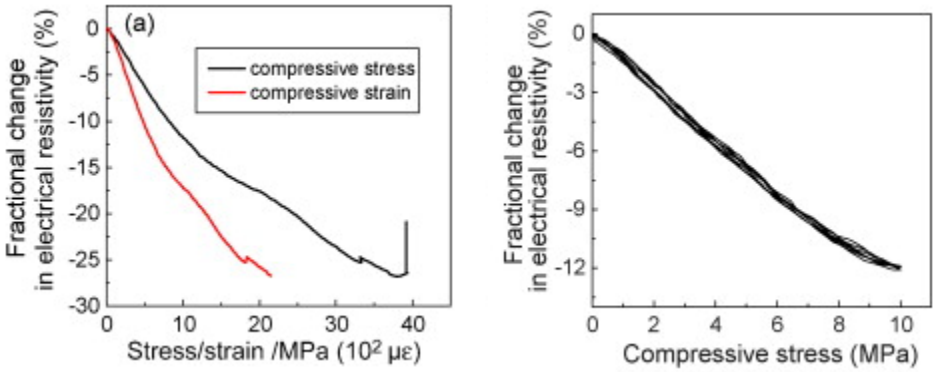

Figure 18: Change in resistivity for a static (a) and dynamic (b) case [47]

Li et al. [15] showed that samples with conductive filler percentage in the percolation threshold showed highest sensitivity to applied strain, as compared to two samples which had conductive filler percentages greater than the percolation threshold. The mechanism of conductivity, which was stated to be tunneling effect for samples in the percolation threshold, and percolation theory, which was said to dominate conductivity after percolation, were stated as the reasons for the difference in sensitivity.

Studies with carbon black and cement composites and their use shielding against electromagnetic waves has shown that carbon black when used in large quantities decreases the compressive strength of cement paste.

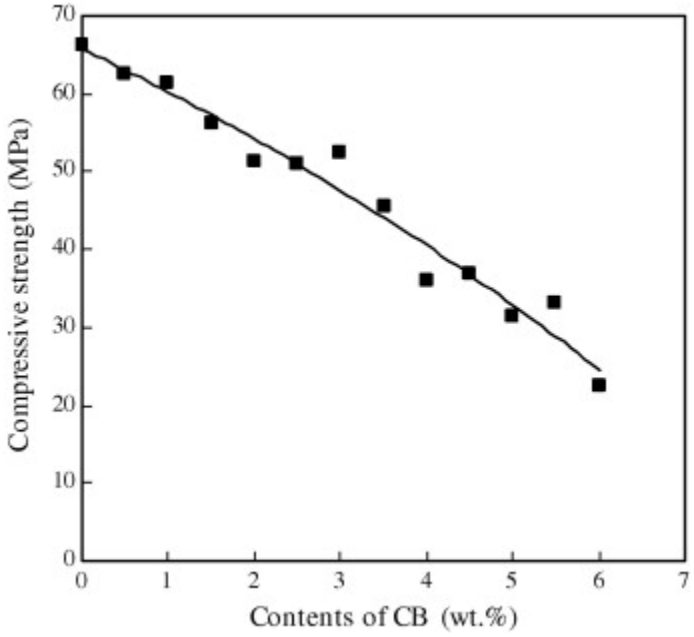

Figure 19: Compressive strength v/s CB loading in weight % [48]

Xiao et al. [48] claimed that the piezoresistivity of carbon fibers differed from that of carbon black filled cement composites, in the sense that CB filled cementitious sensors do not exhibit fiber pull out and reorientation of fibers under applied loading. Instead, they proposed a model that related the deformation applied on a cementitious composite to the internal tunnelling gap between carbon black particles that were dispersed in the cement matrix. An important observation by [49] showed that the initial resistance of cement paste with carbon black was not constant but increased with time and water content, attributed to the polarization effect. These results considered the presence of moisture affecting the initial resistance over time and gave recommendations on sealing the cementitious material from moisture ingress.

However, studies have also shown that medium to low percentage loadings of carbon black actually increase the compressive strength of cement paste and concretes. One study showed that carbon black when added to concrete initially increases the compressive strength of the concrete

mix, due to the densification of the interfacial transition zone, but further increase in the content of carbon black leads to a decrease in the compressive strength due to excess replacement of cementitious mateirals [50].

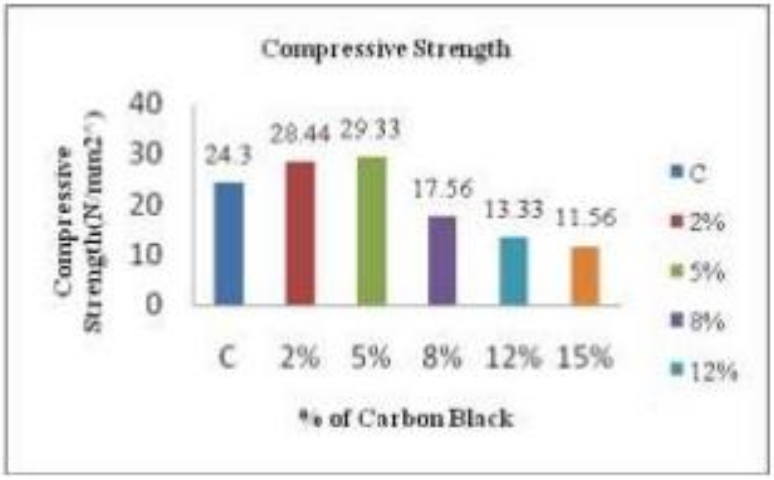

Figure 20: Effect of carbon black on the compressive strength of PCC [50]

This was also seen in a composite of plain portland cement paste and carbon black of varying proportions, where carbon black-cement composites had a higher strength at low concentrations of carbon black but this strength decreased as the percentage of carbon black was increased [31]. Another study investigated the effects of carbon black on the interfacial transition zone between cement and steel reinforcement. The author compared these effects to that of silica fume and noticed that samples containing carbon black proved to be less resistent to crack propagation and had higher values of strain at maximum compressive stress. The study also showed that cement paste with carbon black contained more voids than a comparable percentage of silica fume and the same water to cement ratio [1]. The author cited the possible interaction between carbon black and superplasticizer to the formation of voids in the hardened cement paste microstructure.

The use of two immiscible polymer phases has long been viewed as an efficient method of reducing the percolation threshold of conductive composites. In a Polypropylene-Polystyrene two phase polymer, CB was seen to have affinity for the Polystyrene(PS) phase over the Polypropyle phase(PP) [51]. The authors also witnessed the selective localization of carbon black on PBD(Polybutadiene) phases over PS and PP.

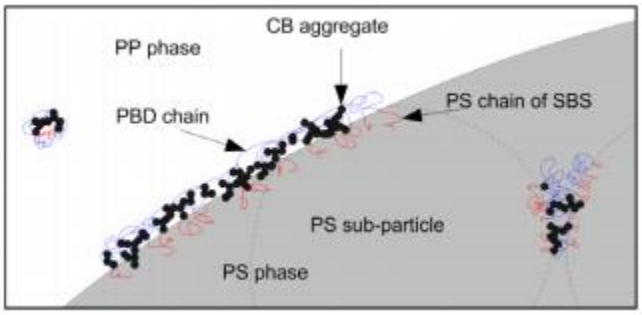

Figure 21: Selective localization of CB on PBD phase of an SBS copolymer [51]

The authors claimed that this agglomeration of CB helped form conductive chains of CB at much lower percolation thresholds, and reported a 40% drop in the percolation threshold on addition of 5% of SBS to a PP/PS polymer.

CHAPTER 3: MATERIALS AND FABRICAION OF SENSORS

3.1. Materials Used

SEBS type Mediprene was obtained from VTC Elastoteknik AB, Sweden (density = 930 kg/m3). It is a petroleum-based block copolymer widely used for medical applications, because of its purity, softness, elasticity, and strength.14 CB type Printex XE-2B (2% ash content and 500 ppm sieve residue 45 μm) was acquired from Orion Engineered Carbons (Kingswood, TX). It is characterized by a high structure (minimum oil absorption 380 cc/100g), which facilitates higher conductivity. The carbon black received was further processed by ball milling it to make finer particles, with the intent of improving dispersion.15 Copper meshes to form the electrodes were acquired from McMaster-Carr (Elmhurst, IL). Portland cement type I/II was locally purchased from Ash Grove Cement Company.

3.1.1. Ball milling of carbon black

Carbon black was ball milled to break down agglomerated particles and hence decrease particle size. This was done with the intention of improving the dispersion of carbon black in the cement and polymer matrix.

Figure 22: Ball mill representation

As explained in the previous chapter, finer filler materials can aid percolation due to the fact that they agglomerate together and have lower inter particle spacing. The carbon black received from Orion Engineered Carbons (Kingswood, TX) was added to the ball mill and milled for 24 hours until fine. It is estimated that 15 hours of ball milling reduced the particle size of CB from an agglomerations of 0.9mm to as small as 47 microns.

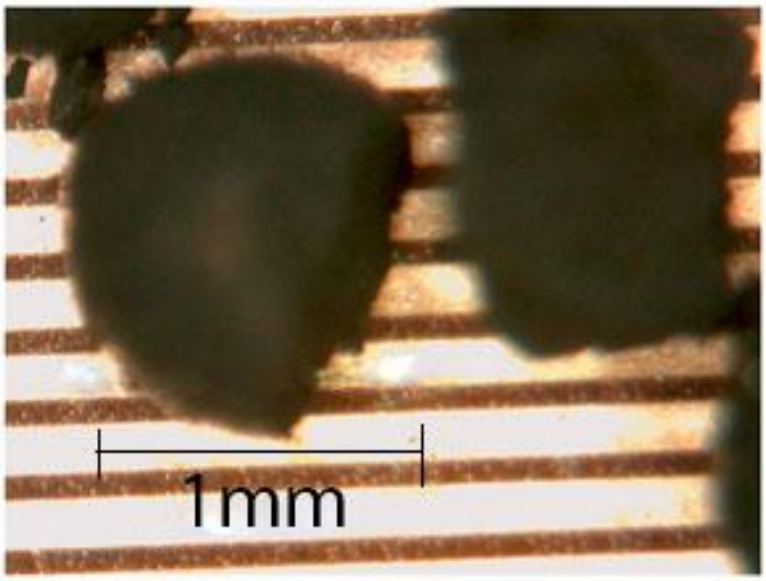

Figure 23: Original CB

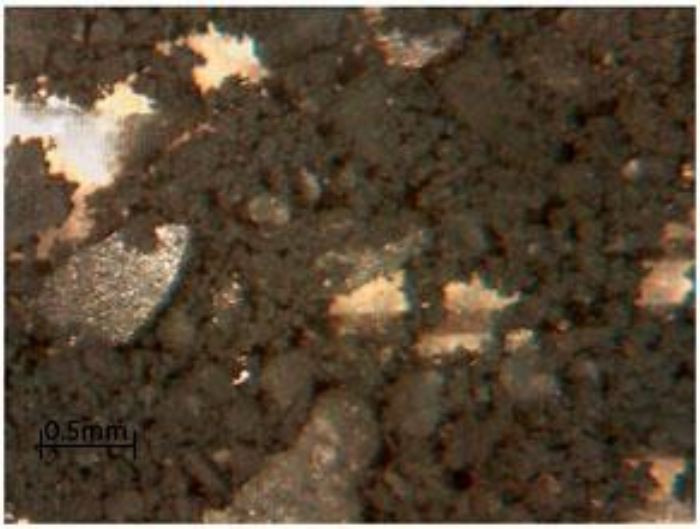

Figure 24: Ball milled CB after 15 hours with extremely fine particles

3.2. Fabrication of Sensors

3.2.1. Fabrication of sensors with carbon black only

One set of sensors were fabricated by using only carbon black as a filler material. The desired amounts of carbon black were weighed and mixed in a blender with the required amount of water needed for a 0.45 water to cement ratio plus an added amount to take into account the absorption of water by carbon black. This mixture was mixed at high shear for 5 minutes in a blender. Cement was then added to this suspension of carbon black and cement in a Hobart mixer. This mix was stirred for 2 minutes at speed 1. Samples were then cast in molds of size 2”x2” with copper electrodes of size stuck to the sides of the molds using pieces of caulk rope. The samples were allowed to cure overnight before being demoulded and allowed to cure in a curing room at 100% relative humidity at 70° C for 7 days. The samples were then allowed to air dry for 4 days before resistivity readings were recorded.

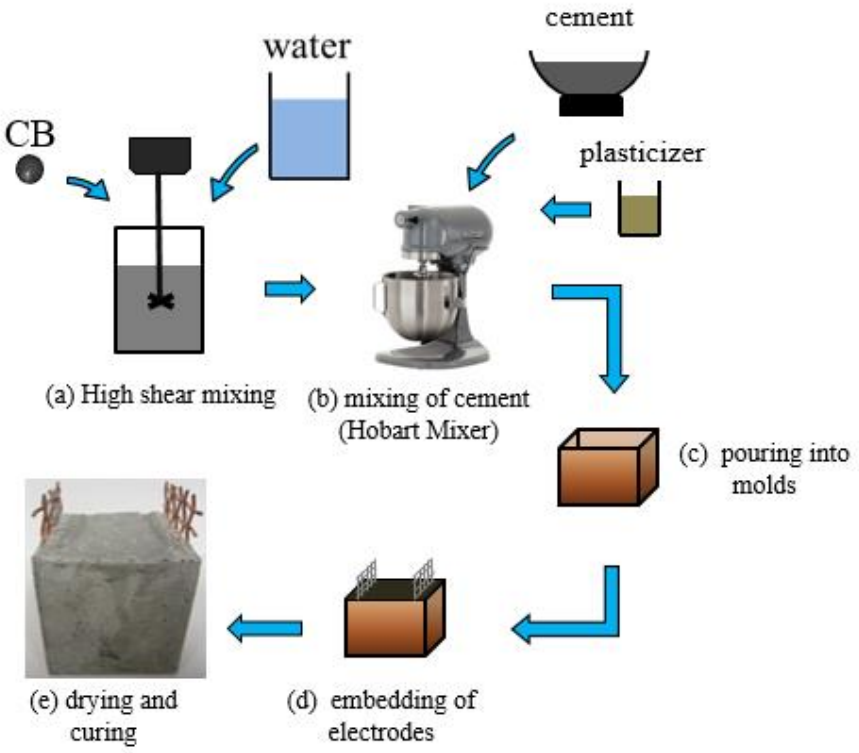

Figure 25: Representation of the fabrication procedure for CB only samples

3.2.2. Fabrication of sensors with carbon black and SEBS

A copolymer SEBS was used in the fabrication of the next batch of sensors with the aim of accelerating the percolation of CB networks within the cement matrix. SEBS polymer obtained in granular form was first dissolved in toluene in the ratio of 60g of SEBS per 500ml of toluene. CB was then added to this solution in the desired proportions before the mixture was sonicated using a sonic tip for 5 minutes. The proportion of CB to SEBS was determined by the amount of CB to be added. Small amounts of CB required 15ml of SEBS to be added while larger volumes of CB needed 30ml of SEBS to be added. Volume fractions in between used 20ml of SEBS solution for every 2” cubic sample. The resulting SEBS-CB conductive paint is insoluble in water, hence needs

a surfactant in order for it to disperse properly in the cement paste. For the fabrication of CBSCS sensors, cement and water are first pre-mixed in the Hobart mixer for 1 minute before the conductive paint and 0.1g of Sodium Lauryl sulphate per 8 cubic inch sample was added to the slurry. This resultant mixture was mixed for 2 minutes on speed 1 of the Hobart mixer. The samples were then poured into molds of 8 cubic inch capacity and were properly compacted to ensure no air voids were present. The samples were covered with a damp cloth and allowed to cure overnight before being demoulded and placed in a curing room at 100% relative humidity and 72 F for 48 hours. The samples were then allowed to air cure to develop polymer microstructure and let water dry out before being tested.

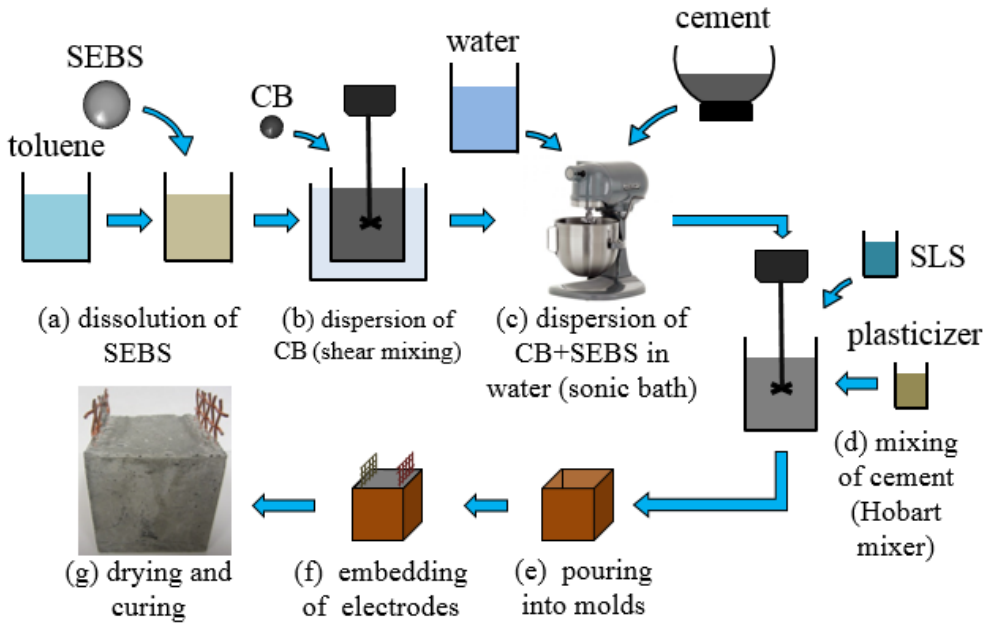

Figure 26: Description of the SEBS Sensor fabrication process

3.3. Mix Proportions for CB and CB with SEBS Sensors

Given below in Table 1 and 2 are the mix proportions of CB only and CB with SEBS sensors

Table 1: CB only samples mix proportions

# of samples	water (g)	CB (g)	cement (g)	plasticizer (ml)	w/c	%CB(vol)
3	293	0.00	651	6	0.45	0.00
3	292	1.65	649	6	0.45	0.18
3	291	3.30	647	6	0.45	0.36
3	290	5.00	645	6	0.45	0.54
3	289	6.65	643	6	0.45	0.71
3	286	9	630	6	0.45	0.96
3	286	12	630	6	0.45	1.25
3	286	15	630	6	0.45	1.60

Table 2: CB with SEBS mix proportions

# of samples	Water(g)	CB(g)	SEBS volume(ml)	Cement(g)	w/c	% CB
3	261	0.00	15	585.90	0.45	0.00
3	261	1.65	15	585.90	0.45	0.18
3	261	3.30	15	585.90	0.45	0.36
3	261	5.00	15	585.90	0.45	0.54
3	261	6.65	15	585.90	0.45	0.71
3	234	9.00	30	519.75	0.45	0.96

CHAPTER 4: TESTING AND EQUIPMENT

4.1. Impedance Measurements

Impedance was measured using an Agilent 4232B LCR meter. All readings for Impedance were measured using a bias of 1000mV at a frequency of 100 KHz. The samples were tested after 7 days of air drying to allow most of the water to evaporate and in the cases of the CB with SEBS samples, the polymer to air cure and its internal microstructure to form.

4.1.1. Impedance v/s strain measurements

Impedance v/s strain measurements were recorded using the Agilent 4323B LCR meter and compressive strain was applied on the sample using an Instron machine with a 50KN capacity. The tests were strain controlled and the strain was applied in increments of 20 micro-strain. Data was logged onto a laptop using a USB interface from National Instruments.

Figure 27: Instron machine used to apply a strain controlled loading on the samples

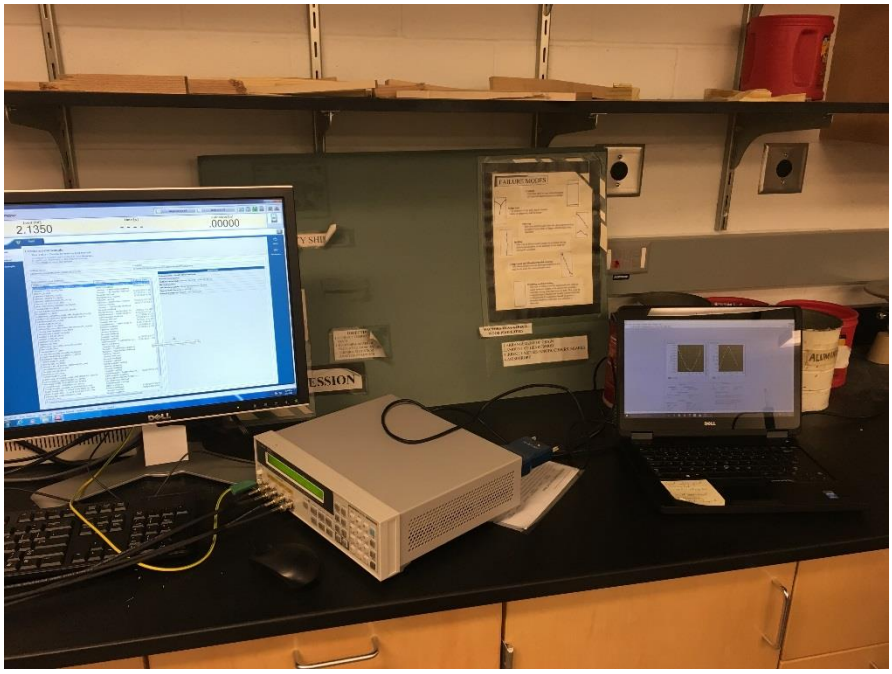

Figure 28: Data acquisition system and laptop used to record the readings

4.2. Measuring the quality of dispersion in the cementitious sensors

In order to have an effective piezoelectric material, the filler material should be uniformly dispersed in the cement matrix to create a homogeneous composite. A good dispersion guarantees a good response to change in strain and reversibility in resistivity. While scanning electron microscopy (SEM) is a common method to determine the level of dispersion in composites, the authors have employed thermography and thermal imaging as an effective alternative, due to the fact that heating will be observed primarily where carbon black particles are situated. Thermal images have the advantage of being able to show a three dimensional view of heating patterns unlike in SEM where only one cross section of the sample can be viewed at any point in time.

The setup involves the cementitious sensors connected to a AC current source stepped down to 60V and placed in an enclosed space, while a thermal camera captures thermal images of the sample as the voltage is applied across the terminals. About one image per second is recorded.

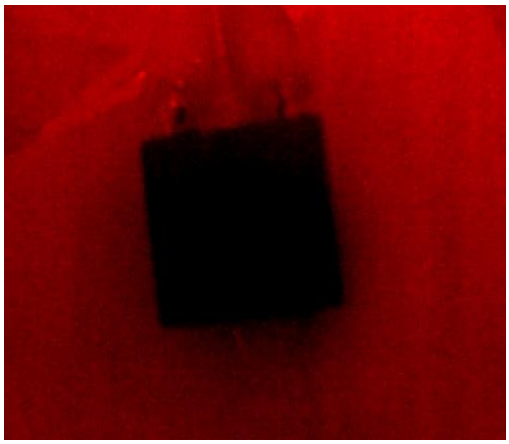

Figure 29: 1.6% CB only before heating

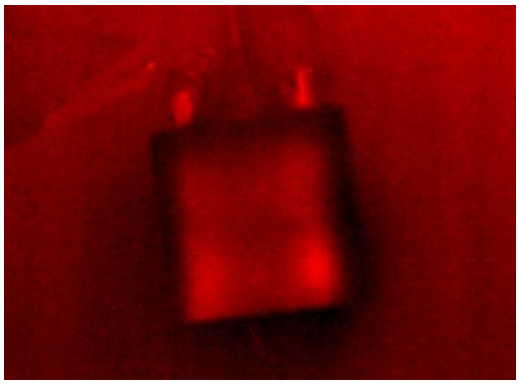

Figure 30: 1.6% CB only after 3 minutes of heating

Figures 29 and 30 show a 1.6% CB only cementitious sensor before and after the 60V potential was applied across its electrodes. The heating can be seen by the brighter areas in the second photo. The heating pattern appeared uniform throughout the height of the sample and thus a good

dispersion is achieved for the 1.6% CB only sample. Since the amount of carbon black in the sample was high, it was also assumed that samples with lower CB % would also show similar dispersion since the mixing process was similar.

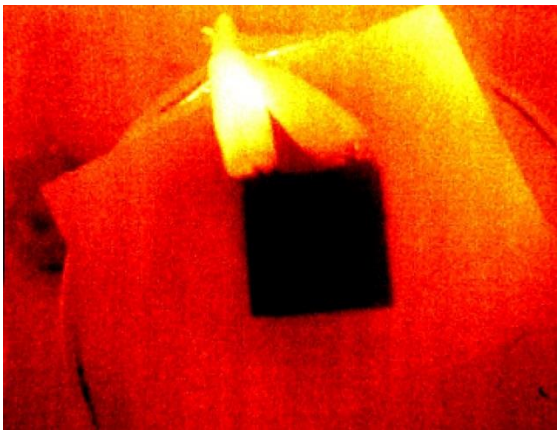

Figure 31: 0.71% CB with SEBS before heating

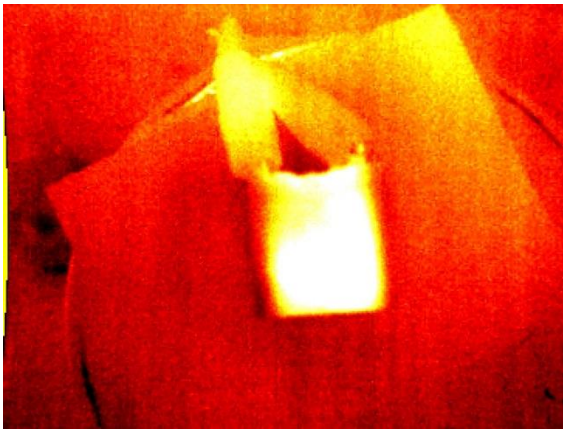

Figure 32: 0.71% CB with SEBS after 3 minutes of heating

Fig 31 and 32 show dispersion of a 0.71% CB with SEBS sensor, and as before, the test shows that a good dispersion was achieved

CHAPTER 5: RESULTS AND DISCUSSION

5.1. Percolation Plots

5.1.1. CB only sensors

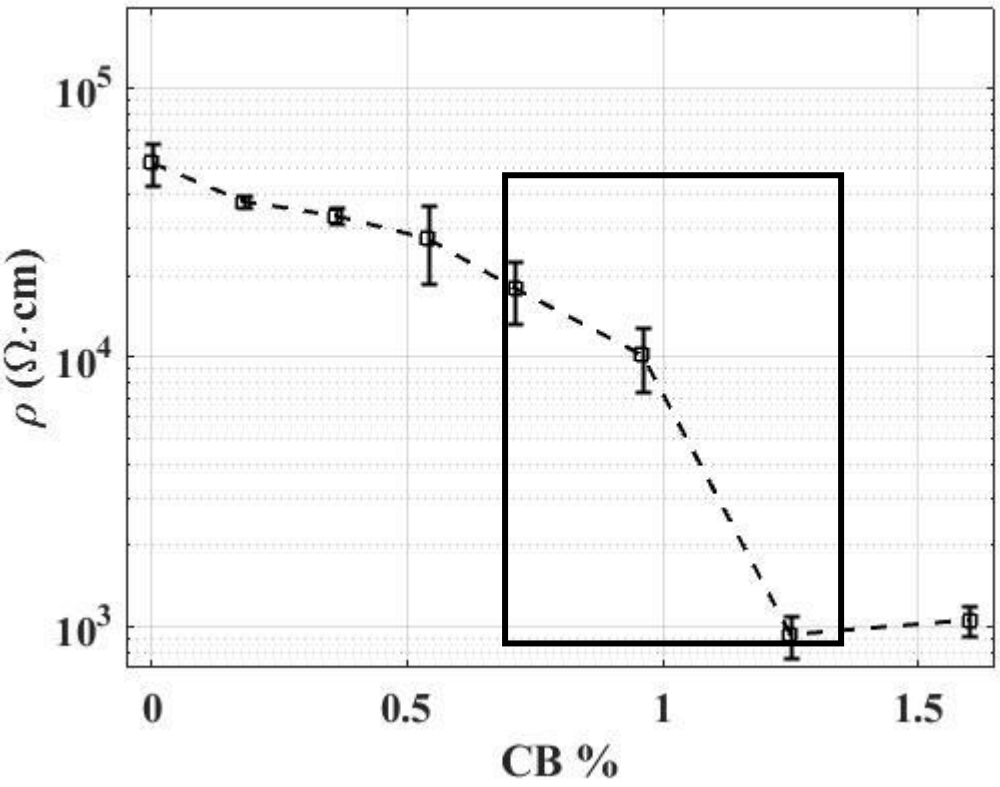

Figure 33: CB only percolation

Figure 33 shows the percolation of CB only specimens with increasing CB filler percentage. As expected, at low filler concentrations, change in resistivity is minimal and decreases sharply as volume of carbon black added increases. The percolation threshold for the CB only samples is between 0.71% and 1.25% CB% by volume.

5.1.2. CB with SEBS sensors

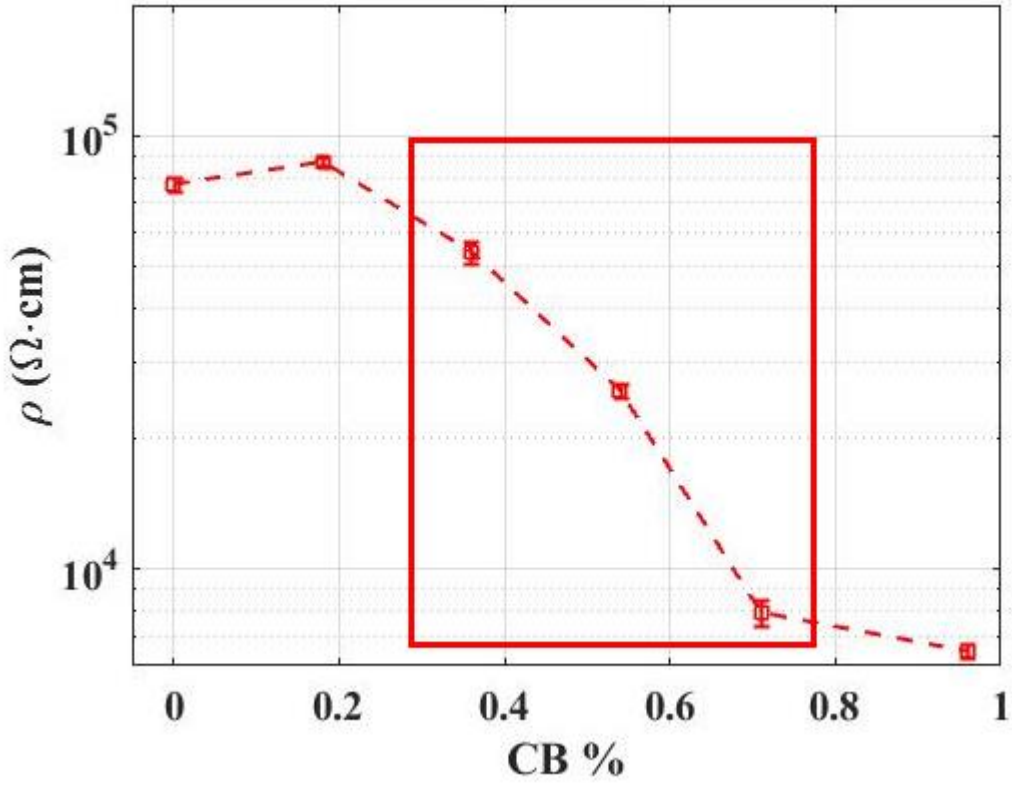

Figure 34: CB-SEBS percolation

The samples containing CB pre-dispersed in SEBS show a similar shape of the percolation curve, however the graph shows that percolation occurs between 0.36% and 0.71%. This shows that SEBS can be used to accelerate percolation as explained in the previous chapters.

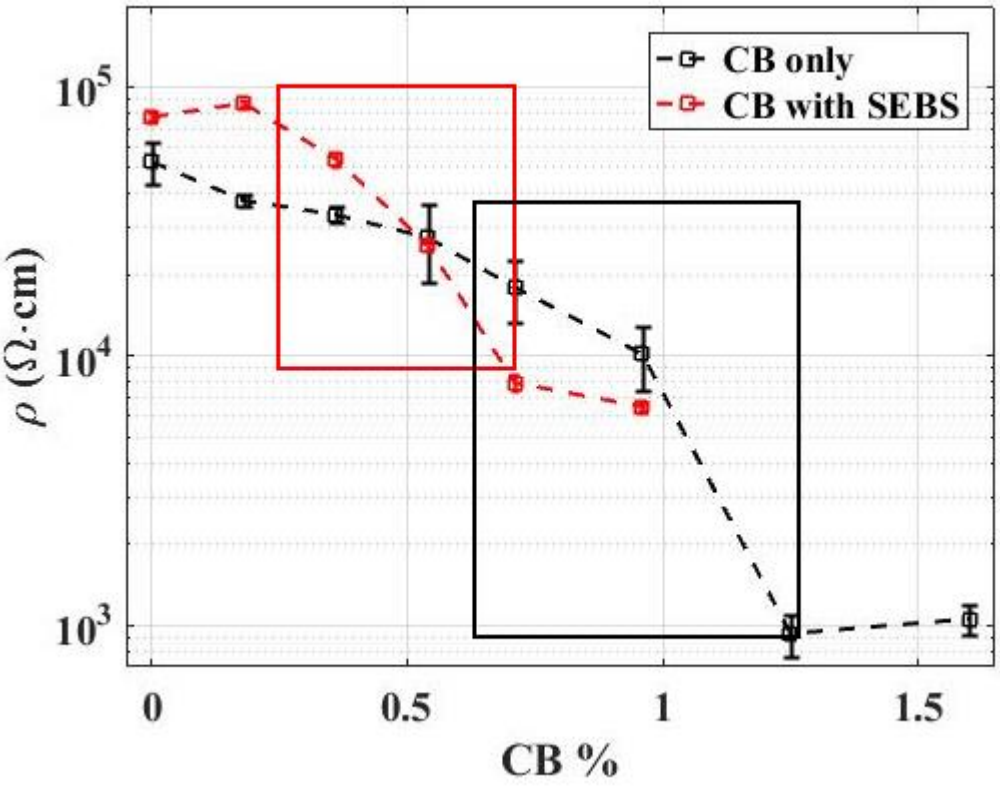

Figure 35: Combined percolation curves of CB only and CB with SEBS

5.2. Effect of SEBS Loading on the Electrical Signal of Cementitious Sensors

Samples were also cast with a constant loading of CB while varying the amount of SEBS to determine the effect of polymer on the conductivity of the cementitious sensors. 0.54% samples of CB with varying loadings of SEBS were prepared and their electrical impedance was recorded.

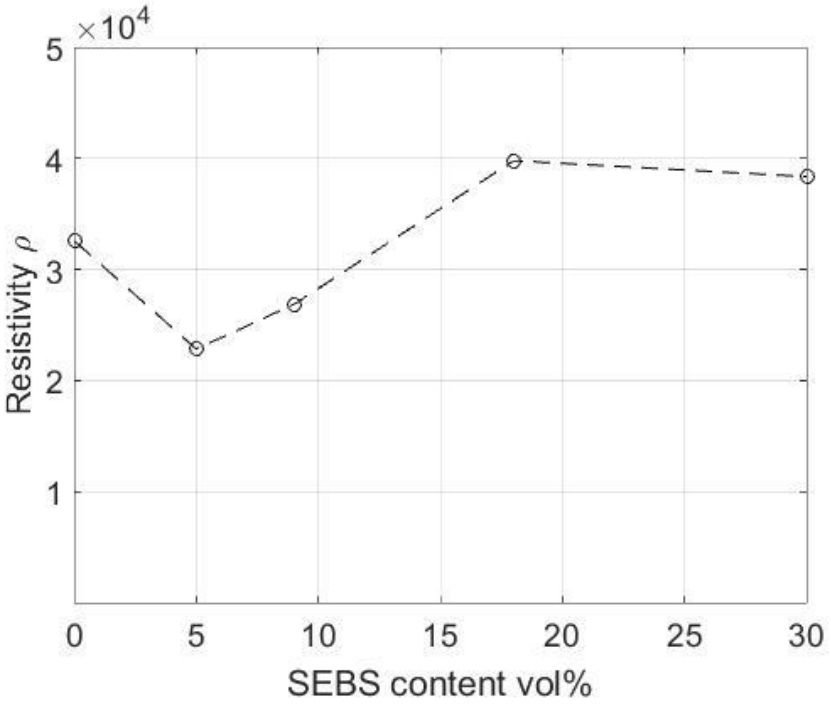

Figure 36: Resistivity v/s SEBS content for constant CB at 0.54% loading

Fig 36 shows that SEBS increases the resistivity of the cementitious sensors as expected, since polymers are good insulators. As loading is increased, the impedance increases as well. The optimum amount of SEBS was chosen to be 9% for samples under 0.71% CB loading. 0.96% samples were loaded with 30% SEBS to help facilitate dispersion. The sample with CB only was not yet conductive despite low impedance, being situated before percolation as seen from the plot of CB content v/s resistivity for CB only samples in fig 36. The resistivity of 0.54% CB only samples becomes steady at loadings above 18%.

5.3. Electrical Response to Applied Loading

The main purpose of the study was to fabricate sensors that percolate faster and prove to be effective at measuring the change in electrical properties of the composite on the application of external strain.

5.3.1. Impedance v/s strain

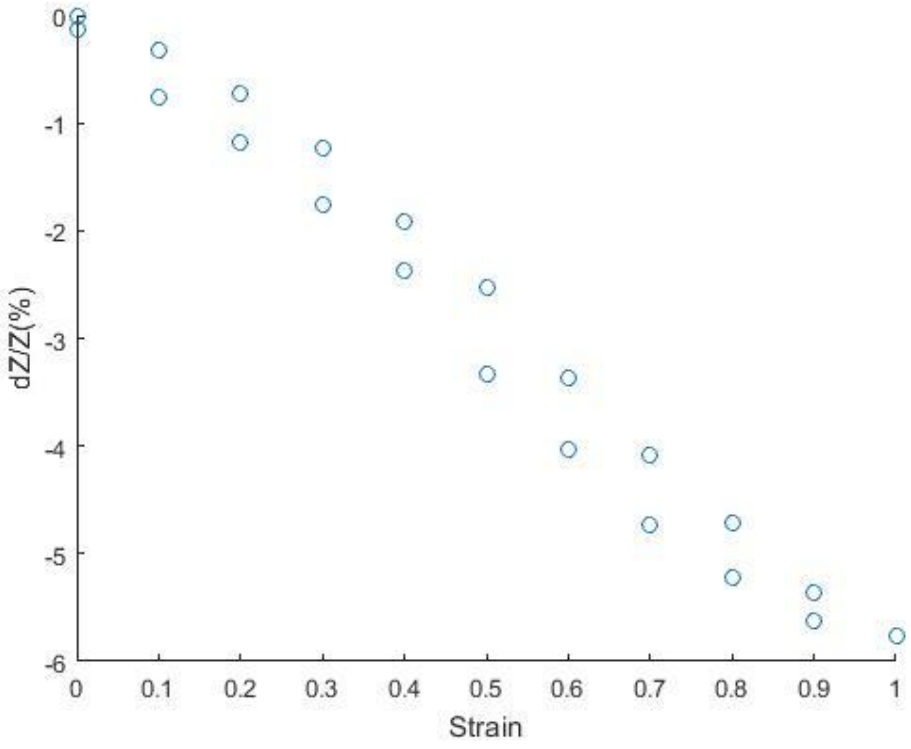

Figure 37: Percent change in Impedance v/s strain for 0.96% CB only samples

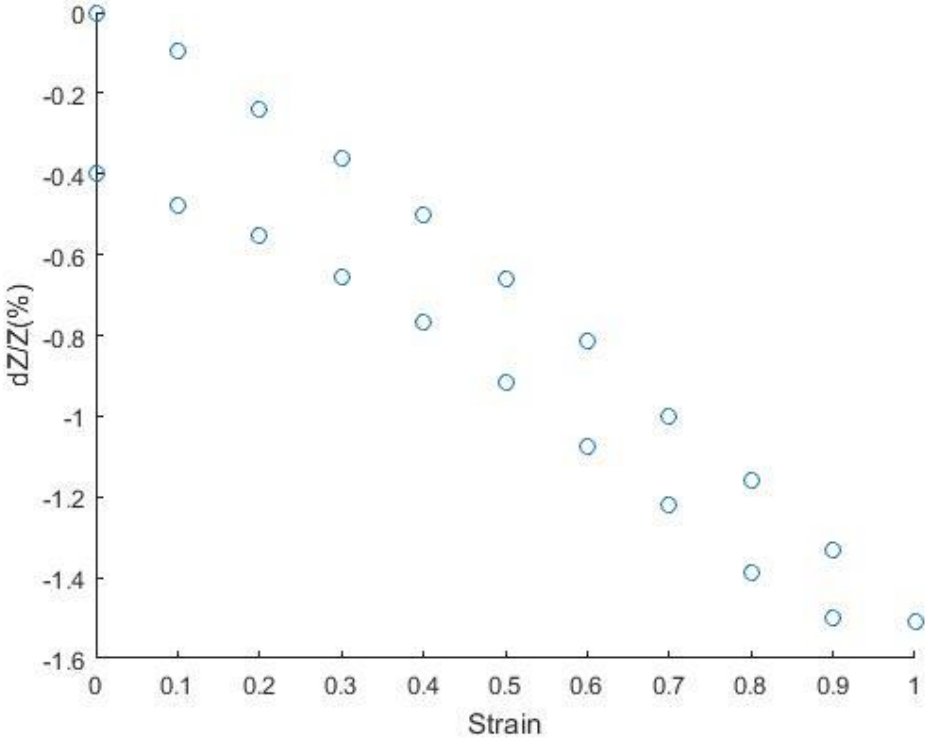

Figure 38: Percentage change in Impedance v/s strain for 0.54% CB with SEBS samples

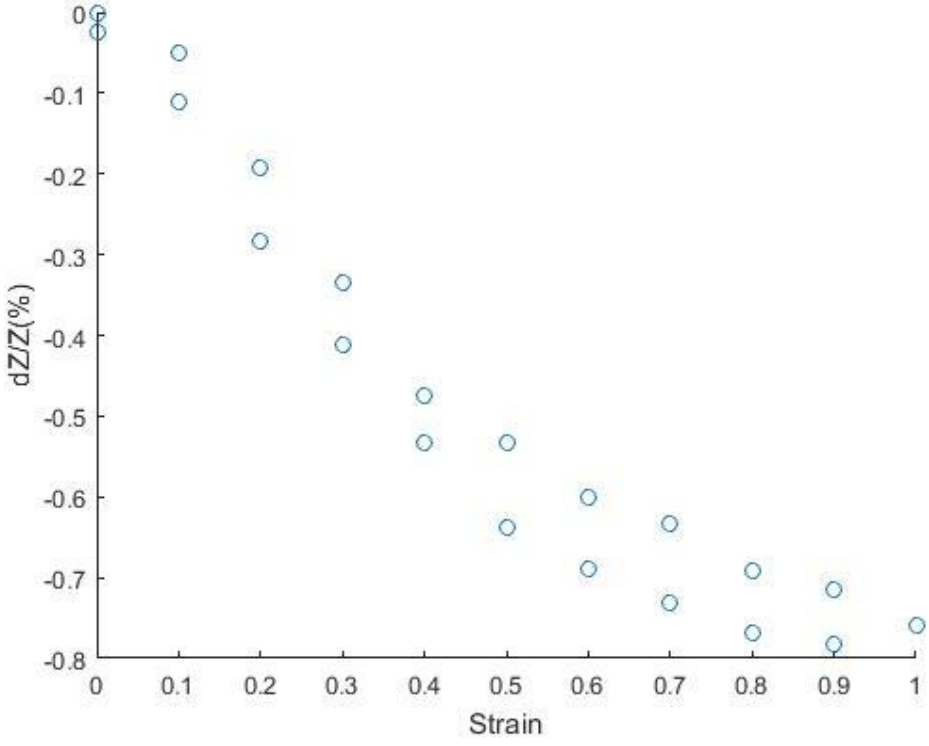

Figure 39: Percentage change in strain for 0.71

CB only samples showed an almost linear and reversible change in Impedance when external strain was applied. The hysterisis was minimum in the case of 0.96% and was slight in the case of 1.25%. Samples with SEBS showed more nonlinearity and also more hysterisis than the CB only samples.

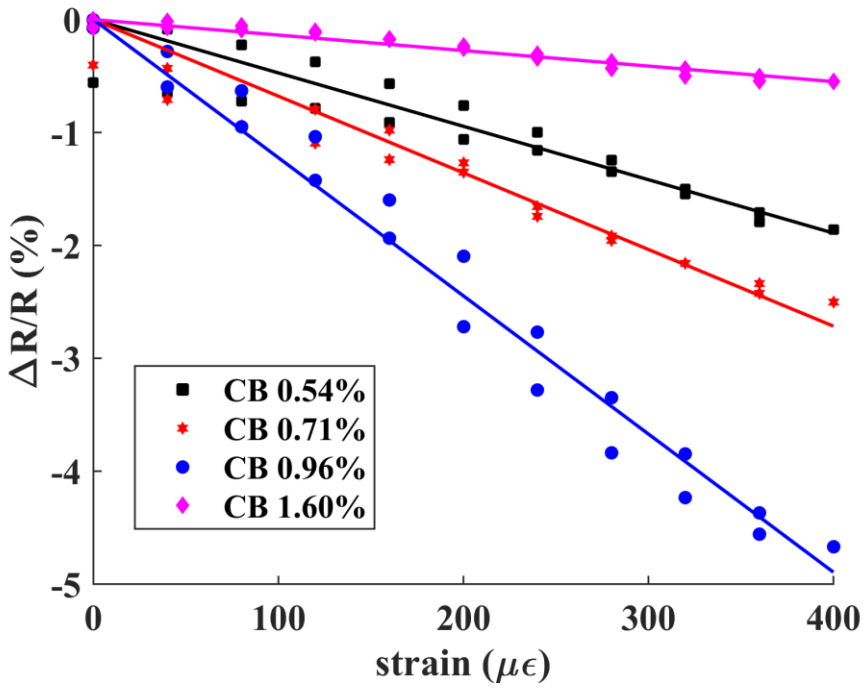

Figure 40: Strain v/s Impedance for CB only samples before, within and after the percolation threshold

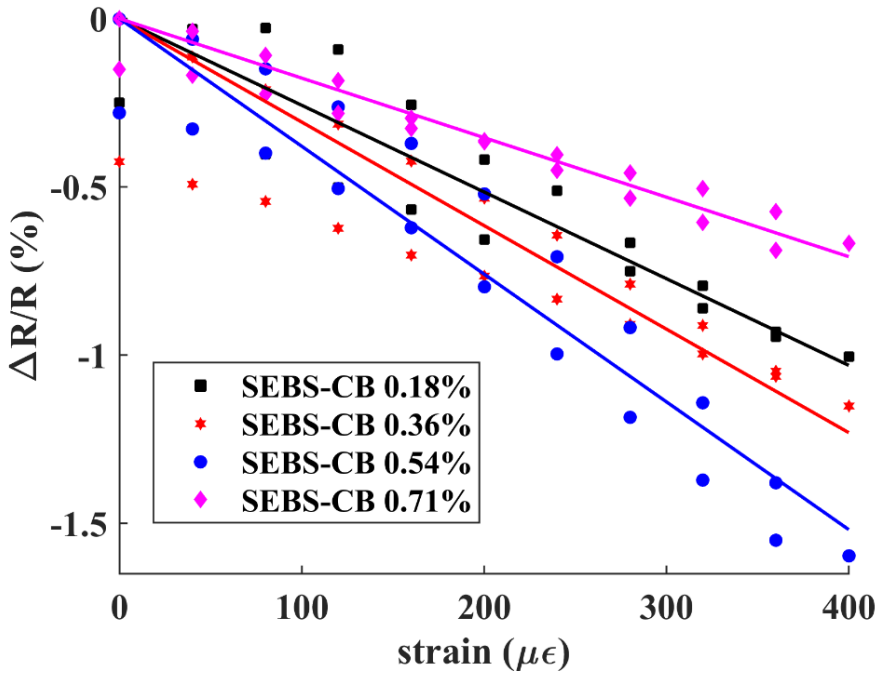

Figure 41: Strain v/s Impedance for CB with SEBS samples before, within and after the percolation threshold

Table 3: Gauge factors of CB and CB with SEBS sensors

Loading	SEBS-CB dR/R /e	CB dR/R /e
0.18%	25.8	N/A
0.36%	30.8	N/A
0.54%	38.0	47.3
0.71%	17.7	82.5
0.96%	N/A	178
1.60%	N/A	17.0

From both the graphs it can be seen that the samples that are situated in the percolation threshold are generally more sensitive to strain than those which are situated outside the percolation threshold, both before and after percolation. It was seen that samples before percolation did not show a very linear response to applied strain while the response to strain was generally better in those samples which were situated both in the percolation threshold and after the percolation threshold. As explained in chapter 2, samples that are situated in the percolation threshold are usually more sensitive to strain simply because the conductive particles have only begun forming chains, so any applied strain reduces the inter particle width. From the tunneling equation we see that the relationship between the conductivity of the composite and the interparticle width is an exponential one, thus a decrease in the particle distance leads to a large increase in the conductivity. In the case of the CB with SEBS samples, nonlinearity was seen more in the 0.54% sample which was situated in the percolation threshold than the 0.71% sample, although both samples showed a degree of nonlinearity greater than the CB only samples. Samples with CB and SEBS showed a slightly larger hysterisis and were significantly less sensitive than the CB only samples. The hysterisis is possibly due to the fact that the polymer needs to relax completely before readings would be perfectly linear.

5.4. Cyclic Loading with Constant Strain

Repeated cyclic loading tests on the samples showed that the CB with SEBS samples gave linear and reversible responses after about two cycles, and even the samples with CB only needed one cycle in order to show fully reversible and linear changes in impedance with strain. The plots for strain v/s impedance are shown below.

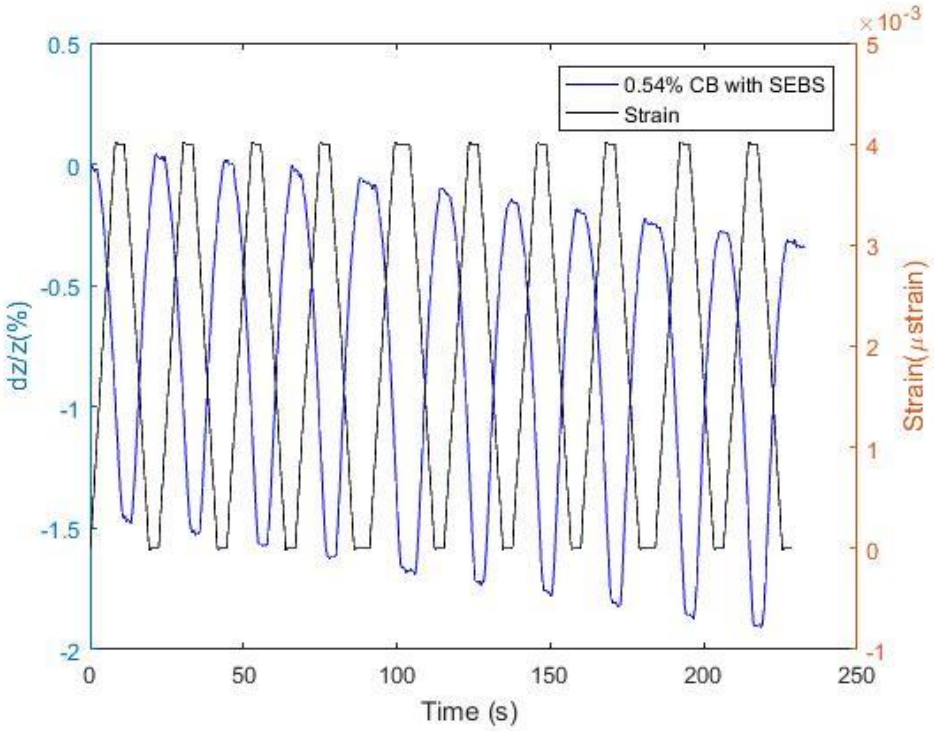

Figure 42: Impedance v/s time for 0.54% CB with SEBS

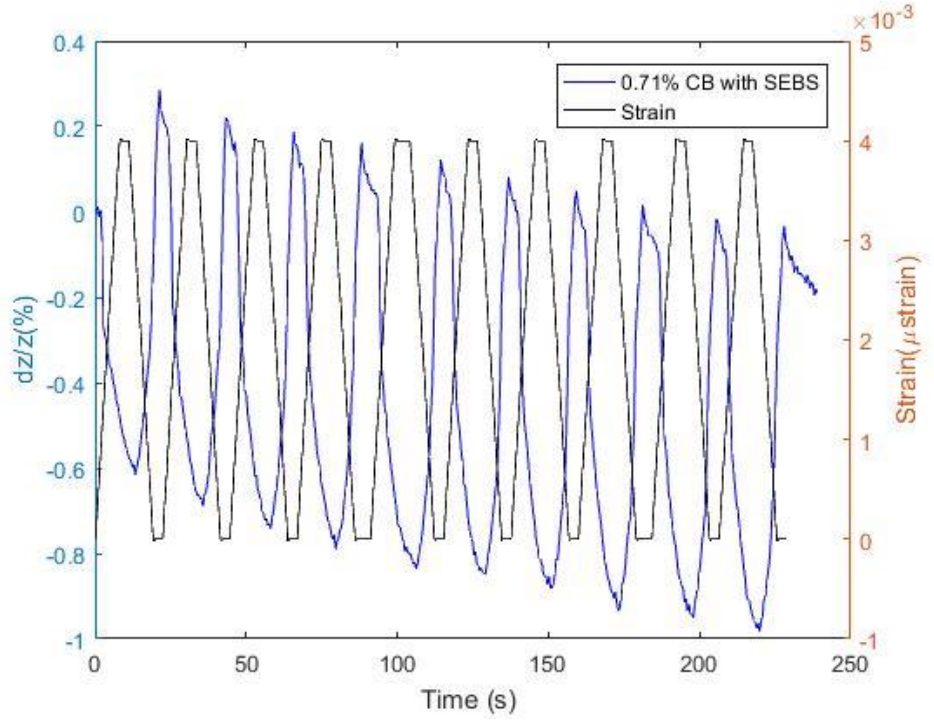

Figure 43: Percent change in Impedance v/s time for 0.71% CB with SEBS

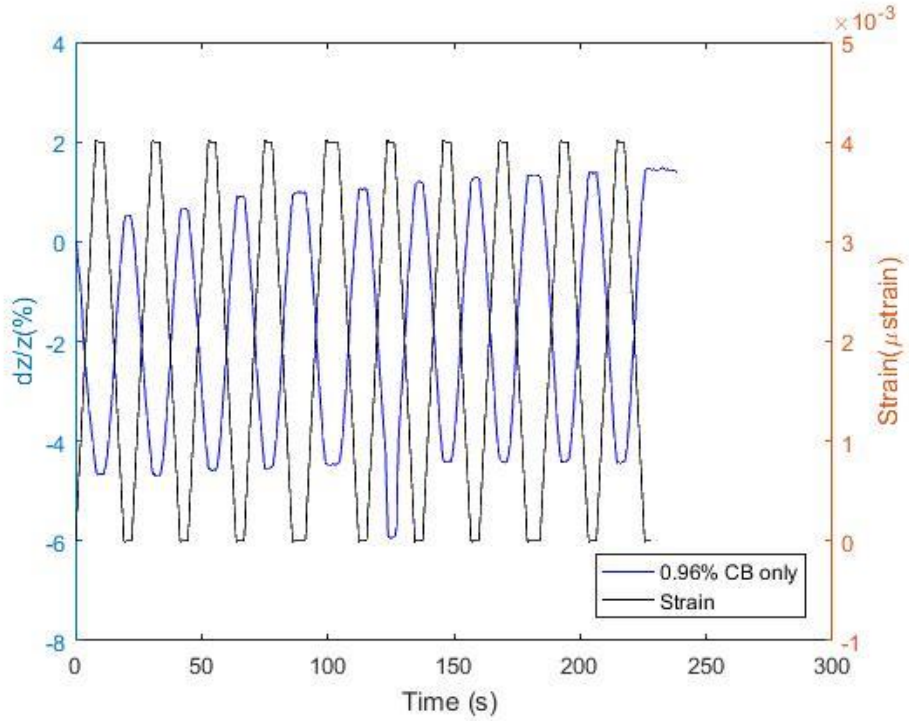

Figure 44: Percent change in impedance v/s time for 0.96% CB only

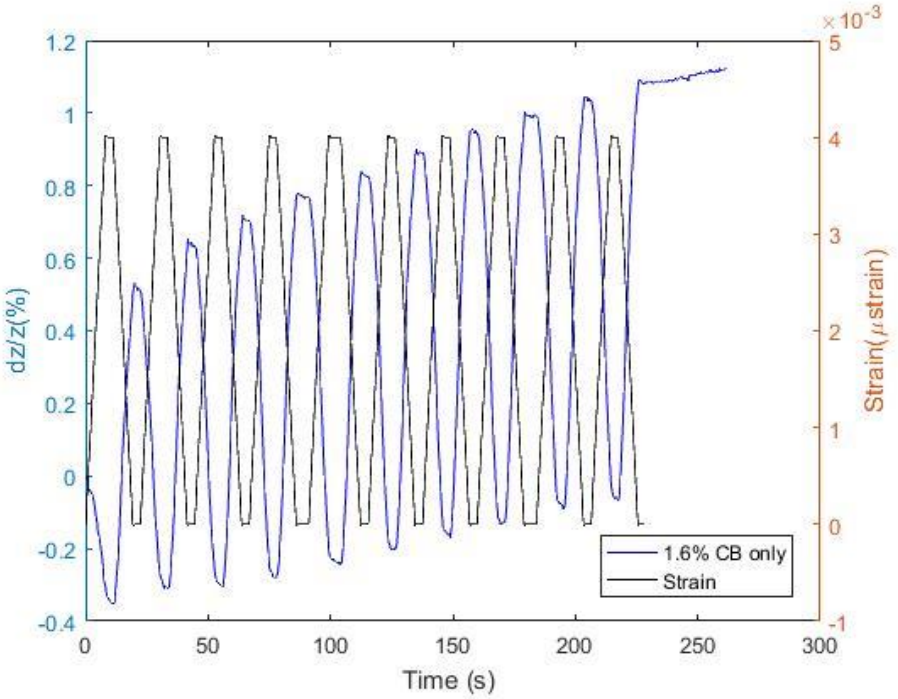

Figure 45: Percent change in impedance v/s time for 1.6% CB only

The repeated cyclic loading results show that both the CB only and CB with SEBS samples produce repeatable results. The samples of CB with SEBS need one cycle for the polymer to fully relax before the results can be repeatable. In some cases, the Impedance increases to a positive percentage fraction of the original value due to the elastic nature of the polymer while it relaxes, most prominently seen in figure 43 with 0.71% CB with SEBS, causing the Impedance to increase more sharply. Once fully relaxed, the samples show good repeatability.

5.5. Cyclic Loading with Varying Strains:

When the samples were loaded with varying strains, the samples with CB only did not respond as well to changing strains as the samples with SEBS. The same samples which were subjected to a 400με load were now subjected to loading from 200με to 400 με after 5 cycles. This was done to determine the effect of increasing the loading on both the CB only samples and the SEBS samples.

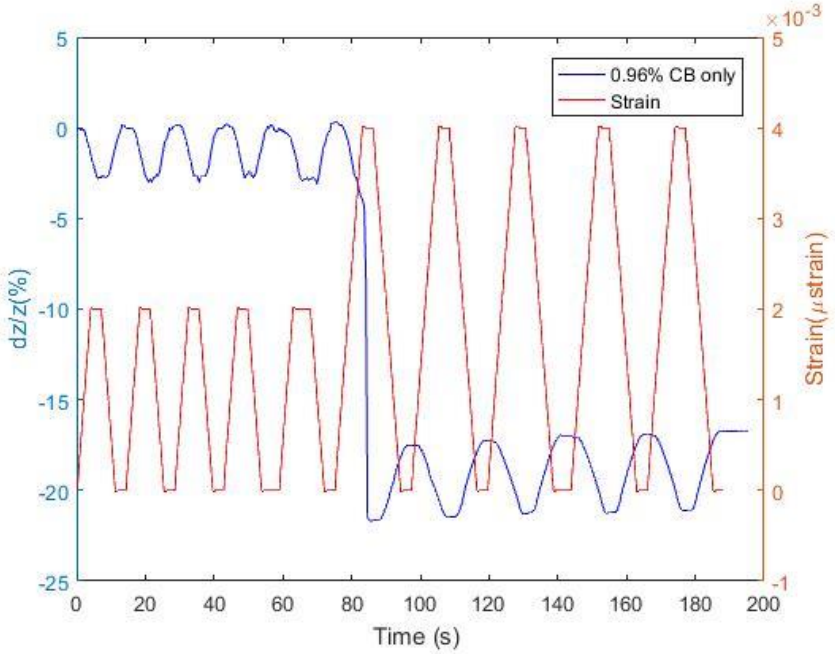

Figure 46: Impedance v/s Time for 0.96% CB only sample

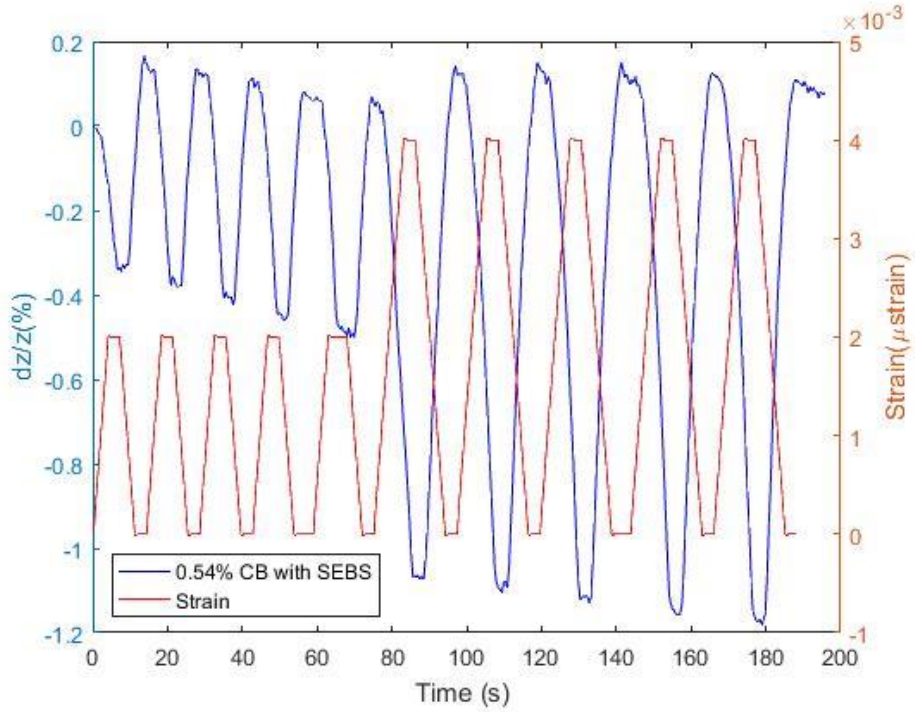

Figure 47: Change in impedance and strain v/s time for 0.54% CB with 9% SEBS

From the Impedance v/s time data for the CB only samples, it can be seen that in the case of the 0.96% CB only samples, the Impdeance values showed good repeatability for values upto 200με but showed an irreversible decrease for 0.96% CB only. The data for 0.54% CB with SEBS showed that the changes in impedance were proportional to the applied strain throughout the loading cycles.

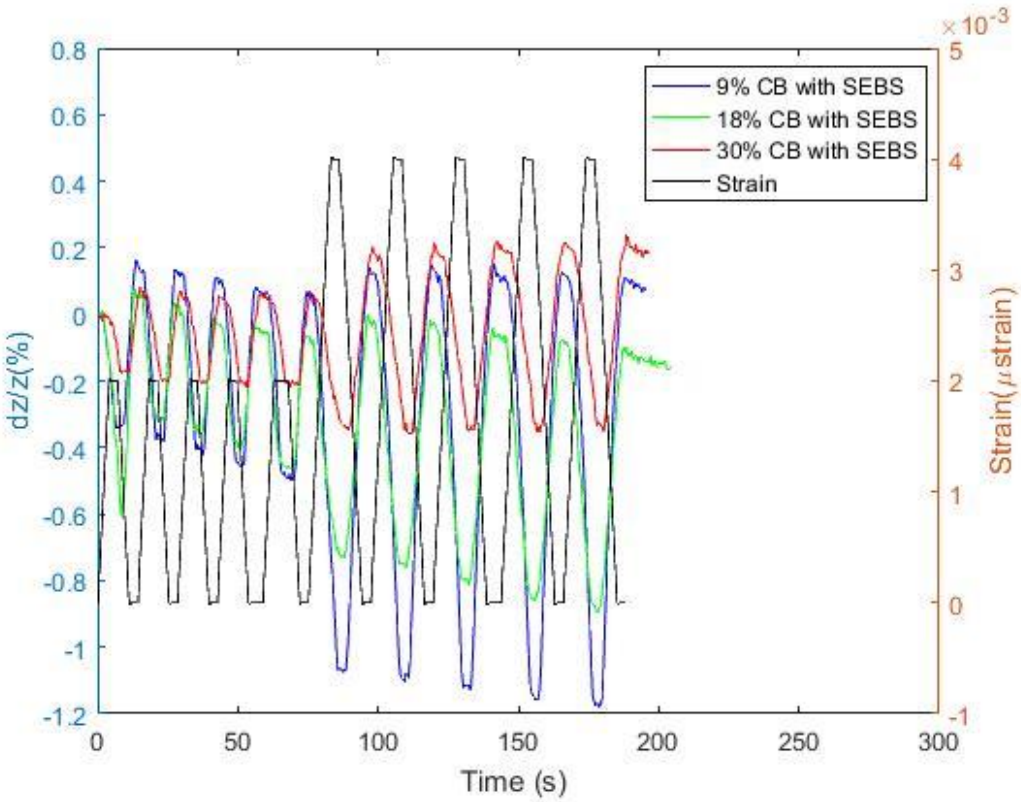

Figure 48: Time v/s Impedance for 0.54% CB with SEBS sensors with 9%, 18% and 30% SEBS respectively.

To determine the effect that the amount of SEBS had on the repeatability and hysterisis of the sensors, three samples with varying amount of SEBS were tested under repeated cyclic loading for 10 cycles. The strain was increased from 200με to 400 με after 5 cycles. The sample with 9% SEBS was the most sensitive, which agrees with the results from the CB only samples, that show that CB only samples are more sensitive in general. As the amount of SEBS is increased, the sensitivity gradually decreases. The sample with 18% SEBS sees the least overall change in the final value of Impedance, but if the initial cycle is ignored because the polymer must be allowed to be pre strained, the 9% SEBS sample has the best repeatability. In all cases however, the presense of SEBS caused the impedance to drop when no strain was being applied on the samples, This can be seen from the gradual decrease in the preaks for all 3 samples. The samples

were all fatigued and preloaded to 300με before testing in order to simulate real loading conditions and also to ensure the sample would be at full strength for the testing. Another reason for the increase or decrease in the impedance with cycles is because only two probes were used in sample casting. Two probe testing was simpler in the case of cementitious sensors but did not take into account the potential damage of the electrodes while loading and unloading which could cause a permanent chance in the impedance readings. 4 probe methods are usually employed where the contact resistance is low and resistance of the cables are comparable to the resistance of the sample to be measured.

5.6. Impedance v/s Temperature

The variation of Impedance of the cementitious sensors with temperature is extremely important in the application of these cementitious composites for the real time health monitoring of large scale infrastructure.

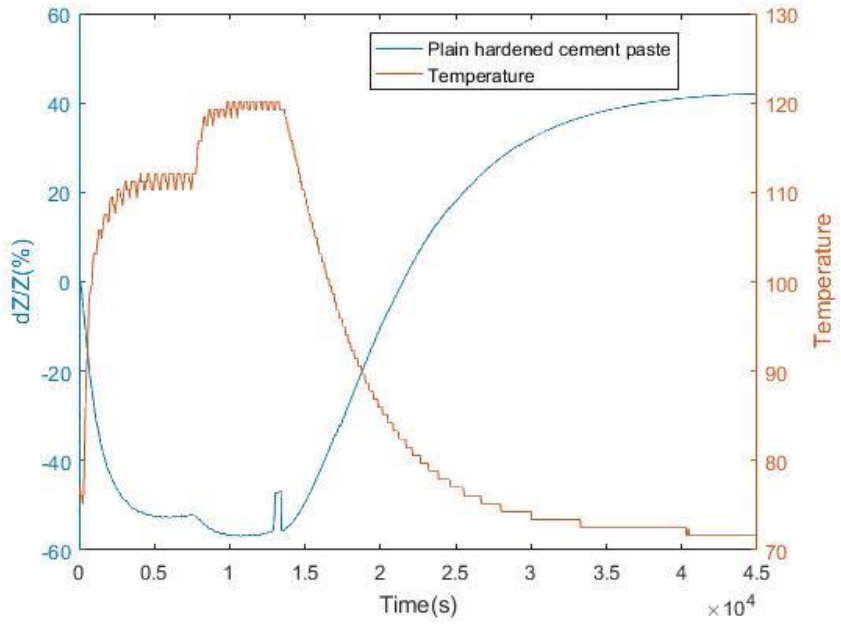

Figure 49: Change in Impedance with time for varying temperature (Plain cement paste)

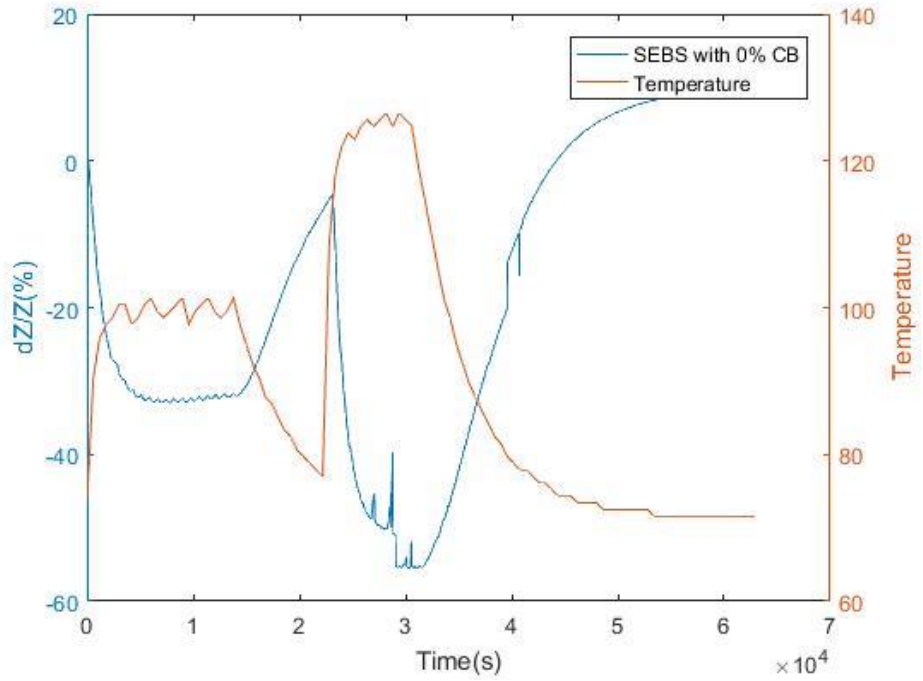

Figure 50: Percent change in Impedance with time for varying temperature (Cement paste with SEBS)

The plots in Fig 45 and Fig 46 show that the plot of temperature with time is almost a mirror image of the impedance variation of impedance with time for the sample with cement paste and SEBS only, except for a few peaks in the impedance v/s time plot. The decrease in resistivity is due to a decrease in activation energy for the conductivity process and change in the pore water fluid ionic concentration. The data from the plain cement samples show that the final impedance value is much more than the initial value. The final value for SEBS is about the same as the initial value with a much smaller permanent change.

5.7. Compressive Strength

To determine the effects of SEBS and CB on the compressive strength and hence the hydration of cement particles, 2”x2” cubes with CB only and CB with SEBS were prepared for testing both short term 7 day strength and long term 28 day strength. The samples were allowed to cure for 7 or 28 days in 100% relative humidity according to ASTM C39. The

samples were then crushed using a compression-testing machine. The compressive strength as well as the peak load before failure for the samples was recorded

The compressive strength of the samples are listed in the table below:

Table 4: Compressive strength of Samples with Cement only

CB %	SEBS%	Peak load (lbs)	Peak Strength (psi)	Mean strength (psi)
		27590	6898	
0%	0%	27230	6807	6904.33
		28032	7008	
		22930	5732.5	
0.54%	0%	30920	7730	7369
		31260	7815	
		7030	1757.5	
0.71%	0%	24420	6105	6162.5
		24880	6220	

Table 5: Compressive strength of Cement samples with SEBS

CB%	SEBS %	Peak Load	Peak Strength	Mean Strength
		22760	5690	
0.54%	9%	18960	4740	5406.25
		20490	5122.5	
		21570	5392.5	
0.71%	9%	21190	5297.5	5345
		12680	3170	

As can be seen from Table 2, cementitious sensors with carbon black only had higher strengths but had much more damage on breaking as compared to the samples with SEBS and the control samples with plain cement paste, as observed in Figures 50 and 51. A reason for the difference in failure could be because the SEBS controls cracking in the cement paste despite not providing considerable compressive strength. SEBS has a specific gravity of 0.89 and hence a 9% replacement of cementitious material by volume results in a drop in compressive strength, since SEBS is not cementitious in nature. Carbon black is seen to actually increase the compressive strength of cement paste for low percentages (0.54%) while higher fractions of Carbon black show a decrease in compressive strength.

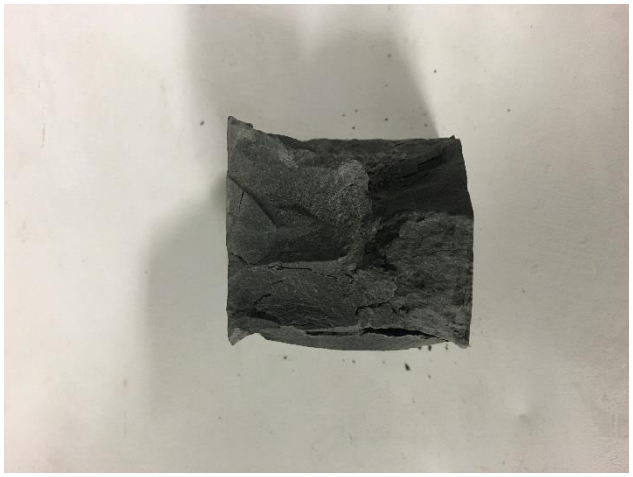

Figure 51: Broken specimen of CB only showing all sides broken

Figure 52: Broken specimens of CB with SEBS showing much less damage at failure

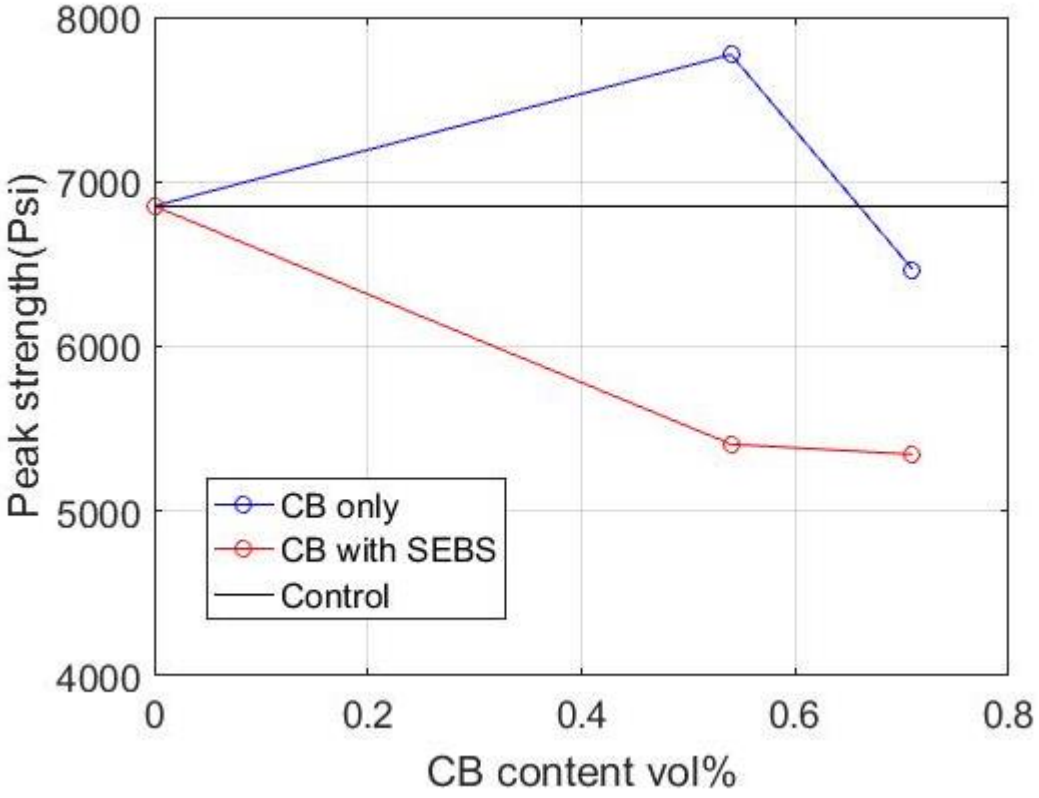

Figure 53: Strength v/s CB content for CB samples with SEBS

Figures 52 and 53 show the decrease in strength with the addition of SEBS to cement. The observed drop in compressive strength when compared to CB only samples can be traced to the SEBS solution used in the conductive paint. Toluene is used to dissolve SEBS to make the polymer solution, and since toluene is highly volatile, evaporation of toluene as the samples cure causes voids to form in the cement paste on hardening. Also likely to cause a drop in strength is the replacement of cement with conductive paint, which is much more in the case of samples with CB and SEBS. Polymer solution could also coat cement grains and inhibit hydration. The effects of SEBS and toluene on the hydration of cement paste needs to be studied further, which would surely provide solutions to tackle the observed loss in strength.

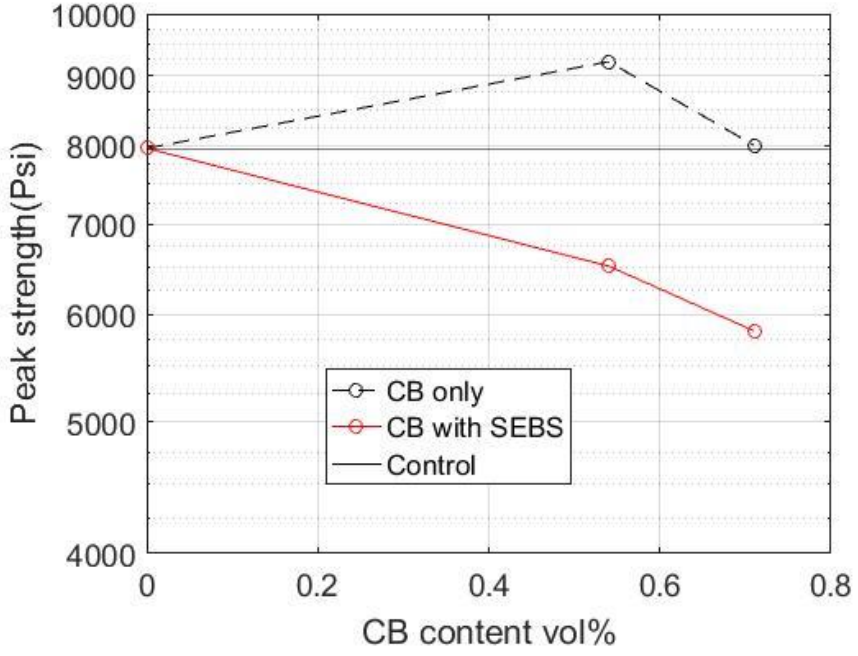

Figure 54: 28 days compressive strength

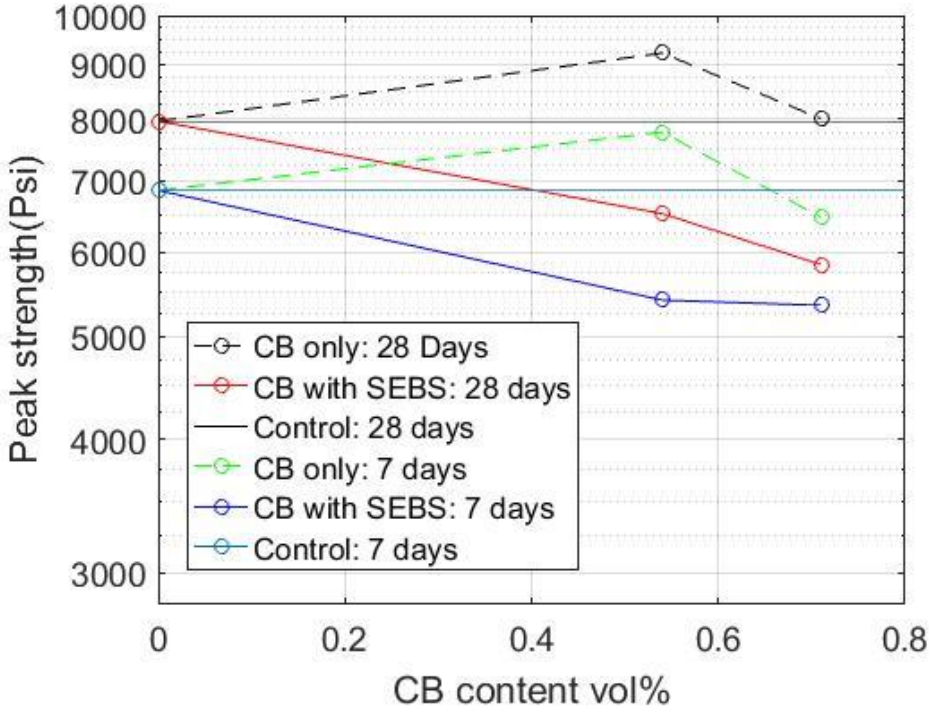

Figure 55: 7 days v/s 28 days compressive strength

Table 6: Strength gain from 7 to 28 days

Strength gain					
CB (% vol)	SEBS (% vol)	7 day avg (psi)	28 day avg (psi)	Increase (psi)	%increase (%)
0	0	6852.50	7958.83	1106.33	16.14
0.54	0	7772.50	9170.83	1398.33	17.99
0.54	9	5406.25	6516.67	1110.42	20.54
0.71	0	6466.25	8000.83	1534.58	23.73
0.71	9	5345.00	5837.50	492.50	9.21

Table 6 shows the strength gain from 7 to 28 days shows an almost even increase in strength, almost similar to the control sample, from 7 days to 28 days. However 0.71% CB with 9% SEBS shows the least increase in strength. The 0.71% CB only shows the greatest increase in strength.

CHAPTER 6: CONCLUSIONS AND FUTURE SCOPE

This study has examined the possibility of reducing the percolation threshold of cementitious sensing materials by employing a co-polymer SEBS to disperse CB within the cement matrix. The results obtained in the study have shown that SEBS can successfully reduce the percolation threshold of cementitious sensing materials with CB due to the preferential affinity of CB to one of the immiscible phases of SEBS, enabling the formation of conductive chains faster. The strain sensing characteristics of cementitious materials with CB and SEBS were also studied. The following conclusions were made from the study:

- Specimens containing CB only had a much higher percolation threshold than those with CB and SEBS. This showed that the polymer was successful in reducing the percolation threshold in cementitious composites
- Specimens with SEBS were less sensitive to strain than CB only samples. This was also observed when increasing percentages of SEBS were added to specimens. SEBS being an insulator also increased the electrical impedance of the material.
- Specimens with CB and SEBS performed better under repeated loading and better matched changes in strain during cyclic loading.
- Specimens with CB and SEBS had a lower compressive stress as compared to that with CB only. This was possibly attributed to the fact that SEBS replaces a large quantity of cement for a similar volume and hence the reduction of cementitious material causes a reduction of compressive strength.
- CB only specimens showed much more damage at failure than SEBS possibly because the polymer prevents the propagation of cracks.

- The effect of temperature on the electrical impedance of samples was studied and it was seen that increased temperatures decreased the electrical impedance considerably, possibly due to the change in pore water ionic concentration.

Future work also needs to be done to observe the chance in electrical signal in different moisture conditions and for long-term loadings. These sensors have a good potential to be weigh in motion sensors or even replace conventional strain gauges in large-scale infrastructure. Therefore, a lot more work has to be done as far as the long-term usability of these sensors in detecting strain and damage in structures.

REFERENCES

[1] R. J. Detwiler, "Subcritical crack growth in the cement paste-steel transition zone," *Cem. Concr. Res.*, vol. 20, no. 2, pp. 277–284, 1990.

[2] C. A. Martin, J. K. W. Sandler, M. S. P. Shaffer, M.-K. Schwarz, W. Bauhofer, K. Schulte, and A. H. Windle, "Formation of percolating networks in multi-wall carbon-nanotube–epoxy composites," *Compos. Sci. Technol.*, vol. 64, no. 15, pp. 2309–2316, Nov. 2004.

[3] A. D'Alessandro, F. Ubertini, S. Laflamme, and A. L. Materazzi, "Towards smart concrete for smart cities: Recent results and future application of strain-sensing nanocomposites," *J. Smart Cities*, vol. 1, no. 1, Sep. 2015.

[4] I. Balberg, "A comprehensive picture of the electrical phenomena in carbon black-polymer composites," *Carbon N. Y.*, vol. 40, no. 2, pp. 139–143, 2002.

[5] X. Jing, W. Zhao, and L. Lan, "The effect of particle size on electric conducting percolation threshold in polymer/conducting particle composites," *J. Mater. Sci. Lett.*, vol. 19, no. 5, pp. 377–379.

[6] I. Fortelný, D. Michálková, J. Hromádková, and F. Lednický, "Carbon black-filled PET/HDPE blends: Effect of the CB structure on rheological and electric properties," *J. Appl. Polym. Sci.*, vol. 81, pp. 562–569, 2001.

[7] J. Huang, "Carbon black filled conducting polymers and polymer blends," *Adv. Polym. Technol.*, 2002.

[8] M. Sumita, K. Sakata, S. Asai, K. Miyasaka, and H. Nakagawa, "Dispersion of fillers and the electrical conductivity of polymer blends filled with carbon black," *Polym. Bull.*, vol. 25, no. 2, pp. 265–271, 1991.

[9] F. Gubbels, R. Jérôme, and P. Teyssie, “Selective localization of carbon black in immiscible polymer blends: a useful tool to design electrical conductive composites,” *Macromolecules*, 1994.

[10] M. H. Al-Saleh and U. Sundararaj, “An innovative method to reduce percolation threshold of carbon black filled immiscible polymer blends,” *Compos. Part A Appl. Sci. Manuf.*, vol. 39, pp. 284–293, 2008.

[11] W. Bauhofer and J. Kovacs, “A review and analysis of electrical percolation in carbon nanotube polymer composites,” *Compos. Sci. Technol.*, 2009.

[12] J. Liang and Q. Yang, “Aggregate structure and percolation behavior in polymer/carbon black conductive composites,” *J. Appl. Phys.*, vol. 102, no. 8, p. 83508, 2007.

[13] L. Rejón, A. Rosas-Zavala, J. Porcayo-Calderon, and V. M. Castaño, “Percolation phenomena in carbon black-filled polymeric concrete,” *Polym. Eng. Sci.*, vol. 40, no. 9, pp. 2101–2104, 2000.

[14] F. El-Tantawy, K. Kamada, and H. Ohnabe, “In situ network structure, electrical and thermal properties of conductive epoxy resin–carbon black composites for electrical heater applications,” *Mater. Lett.*, vol. 56, no. 1–2, pp. 112–126, Sep. 2002.

[15] H. Li, H. Xiao, and J. Ou, “Effect of compressive strain on electrical resistivity of carbon black-filled cement-based composites,” *Cem. Concr. Compos.*, vol. 28, no. 9, pp. 824–828, Oct. 2006.

[16] M. Weber and M. R. Kamal, “Estimation of the volume resistivity of electrically conductive composites,” *Polym. Compos.*, vol. 18, no. 6, pp. 711–725, Dec. 1997.

[17] N. Hu, Y. Karube, C. Yan, Z. Masuda, and H. Fukunaga, “Tunneling effect in a polymer/carbon nanotube nanocomposite strain sensor,” *Acta Mater.*, 2008.

[18] H. G. Xiao and H. Li, “Strain sensing property of carbon black filled cement-based composites,” in *Structural Health Monitoring and Intelligent Infrastructure - Proceedings of the 2nd International Conference on Structural Health Monitoring of Intelligent Infrastructure, SHMII 2005*, 2006, vol. 1, pp. 527–530.

[19] J. F. Zhou, Y. H. Song, Q. Zheng, Q. Wu, and M. Q. Zhang, “Percolation transition and hydrostatic piezoresistance for carbon black filled poly(methylvinylsilioxane) vulcanizates,” *Carbon N. Y.*, vol. 46, no. 4, pp. 679–691, Apr. 2008.

[20] B. Chen, K. Wu, and W. Yao, “Conductivity of carbon fiber reinforced cement-based composites,” *Cem. Concr. Compos.*, vol. 26, no. 4, pp. 291–297, 2004.

[21] J. Feng, C. Chan, and J. Li, “A method to control the dispersion of carbon black in an immiscible polymer blend,” *Polym. Eng. Sci.*, vol. 43, no. 5, pp. 1058–1063, May 2003.

[22] A. I. Medalia, “Electrical Conduction in Carbon Black Composites,” *Rubber Chem. Technol.*, vol. 59, no. 3, pp. 432–454, 1986.

[23] J. Wu, C. Song, H. S. Saleem, A. Downey, and S. Laflamme, “Network of flexible capacitive strain gauges for the reconstruction of surface strain,” *Meas. Sci. Technol.*, vol. 26, no. 5, p. 55103, May 2015.

[24] S. Kharroub, S. Laflamme, C. Song, D. Qiao, B. Phares, and J. Li, “Smart sensing skin for detection and localization of fatigue cracks,” *Smart Mater. Struct.*, vol. 24, no. 6, p. 65004, Jun. 2015.

[25] S. Laflamme, L. Cao, E. Chatzi, and F. Ubertini, “Damage detection and localization from dense network of strain sensors,” *Shock Vib.*, vol. 2016, pp. 1–13, 2016.

[26] G. Y. Li, P. M. Wang, and X. Zhao, “Mechanical behavior and microstructure of cement composites incorporating surface-treated multi-walled carbon nanotubes,” *Carbon N. Y.*, vol. 43, no. 6, pp. 1239–1245, May 2005.

[27] F. Azhari and N. Banthia, “Cement-based sensors with carbon fibers and carbon nanotubes for piezoresistive sensing,” *Cem. Concr. Compos.*, 2012.

[28] S. Wen and D. D. . Chung, “Piezoresistivity in continuous carbon fiber cement-matrix composite,” *Cem. Concr. Res.*, vol. 29, no. 3, pp. 445–449, Mar. 1999.

[29] Z. Li, D. Zhang, and K. Wu, “Cement-Based 0-3 Piezoelectric Composites,” *J. Am. Ceram. Soc.*, vol. 85, no. 2, pp. 305–313, 2002.

[30] J. M. Makar, J. C. Margeson, and J. Luh, “Carbon nanotube/cement composites-early results and potential applications,” 2005.

[31] A. O. Monteiro, P. B. Cachim, and P. M. F. J. Costa, “Electrical Properties of Cement-based Composites Containing Carbon Black Particles,” in *Materials Today: Proceedings*, 2015, vol. 2, no. 1, pp. 193–199.

[32] D. D. Chung, “Dispersion of Short Fibers in Cement,” *J. Mater. Civ. Eng.*, vol. 17, no. 4, pp. 379–383, Aug. 2005.

[33] P.-W. Chen, X. Fu, and D. D. L. Chung, “Microstructural and Mechanical Effects of Latex, Methylcellulose, and Silica Fume on Carbon Fiber Reinforced Cement,” *Mater. J.*, vol. 94, no. 2, pp. 147–155, Mar. 1997.

[34] W. . McCarter, G. Starrs, and T. . Chrisp, “Electrical conductivity, diffusion, and permeability of Portland cement-based mortars,” *Cem. Concr. Res.*, vol. 30, no. 9, pp. 1395–1400, Sep. 2000.

[35] V. Zucolotto, J. Avlyanov, and L. H. C. Mattoso, “Elastomeric conductive composites based on conducting polymer-modified carbon black,” *Polym. Compos.*, vol. 25, no. 6, pp. 617–621, 2004.

[36] S. Wen and D. D. L. Chung, “Double percolation in the electrical conduction in carbon fiber reinforced cement-based materials,” *Carbon N. Y.*, vol. 45, no. 2, pp. 263–267, 2007.

[37] T. Yamada, Y. Hayamizu, Y. Yamamoto, Y. Yomogida, A. Izadi-Najafabadi, D. N. Futaba, and K. Hata, “A stretchable carbon nanotube strain sensor for human-motion detection,” *Nat. Nanotechnol.*, vol. 6, no. 5, pp. 296–301, May 2011.

[38] J. Sumfleth, S. T. Buschhorn, and K. Schulte, “Comparison of rheological and electrical percolation phenomena in carbon black and carbon nanotube filled epoxy polymers,” *J. Mater. Sci.*, vol. 46, pp. 659–669, 2011.

[39] S. Wen and D. Chung, “Carbon fiber-reinforced cement as a strain-sensing coating,” *Cem. Concr. Res.*, 2001.

[40] F. Ubertini, S. Laflamme, H. Ceylan, A. Luigi Materazzi, G. Cerni, H. Saleem, A. D’Alessandro, and A. Corradini, “Novel nanocomposite technologies for dynamic monitoring of structures: a comparison between cement-based embeddable and soft elastomeric surface sensors,” *Smart Mater. Struct.*, vol. 23, no. 4, p. 45023, Apr. 2014.

[41] D. Chung, “Piezoresistive cement-based materials for strain sensing,” *J. Intell. Mater. Syst. Struct.*, 2002.

[42] X. Liu, S. Wu, Q. Ye, J. Qiu, and B. Li, “Properties evaluation of asphalt-based composites with graphite and mine powders,” *Constr. Build. Mater.*, vol. 22, no. 3, pp. 121–126, 2008.

[43] S. Wu, L. Mo, Z. Shui, and Z. Chen, “Investigation of the conductivity of asphalt concrete containing conductive fillers,” *Carbon N. Y.*, vol. 43, no. 7, pp. 1358–1363, Jun. 2005.

[44] X. Liu, W. Liu, S. Wu, and C. Wang, “Effect of carbon fillers on electrical and road properties of conductive asphalt materials,” *Constr. Build. Mater.*, vol. 68, pp. 301–306, Oct. 2014.

[45] S. P. Wu, L. T. Mo, and Z. H. Shui, “Piezoresistivity of graphite modified asphalt-based composites,” in *Key Engineering Materials*, 2003, vol. 249, pp. 391–396.

[46] S. WU, X. LIU, Q. YE, and N. LI, “Self-monitoring electrically conductive asphalt-based composite containing carbon fillers,” *Trans. Nonferrous Met. Soc. China*, vol. 16, pp. s512–s516, Jun. 2006.

[47] B. Han and J. Ou, “Embedded piezoresistive cement-based stress/strain sensor,” *Sensors Actuators A Phys.*, 2007.

[48] H. Xiao, H. Li, and J. Ou, “Modeling of piezoresistivity of carbon black filled cement-based composites under multi-axial strain,” *Sensors Actuators A Phys.*, vol. 160, no. 1–2, pp. 87–93, May 2010.

[49] H. LI, H. XIAO, and J. OU, “Electrical property of cement-based composites filled with carbon black under long-term wet and loading condition,” *Compos. Sci. Technol.*, vol. 68, no. 9, pp. 2114–2119, Jul. 2008.

[50] Pv. Selvi, “Carbon Black as an Additive in Conventional Concrete,” *Int. J. Emerg. Technol. Adv. Eng. Website www.ijetae.com ISO Certif. J.*, vol. 9001, no. 3, 2250.

[51] M. H. Al-Saleh and U. Sundararaj, “An innovative method to reduce percolation threshold of carbon black filled immiscible polymer blends,” *Compos. Part A Appl. Sci. Manuf.*, vol. 39, no. 2, pp. 284–293, 2008.